NASA/TM–20230008831

Effects of Strain Rate and Surface Finish on Tensile Properties in High Pressure Hydrogen — A Case Study for LP-DED NASA HR-1

P.S. Chen,[1] M.D. Fullen,[1] M.C. Watwood,[1] B.L Rupp,[1] W.M. Medders,[2] C.C. Katsarelis,[2] and P.R. Gradl[2]

[1]Jacobs ESSCA Group, Huntsville, Alabama
[2]Marshall Space Flight Center, Huntsville, Alabama

June 2023

The NASA STI Program…in Profile

The NASA STI Program collects, organizes, provides for archiving, and disseminates NASA's STI. The NASA STI program provides access to the NTRS Registered and its public interface, the NASA Technical Reports Server, thus providing one of the largest collections of aeronautical and space science STI in the world. Results are published in both non-NASA channels and by NASA in the NASA STI Report Series, which includes the following report types:

- TECHNICAL PUBLICATION. Reports of completed research or a major significant phase of research that present the results of NASA programs and include extensive data or theoretical analysis. Includes compilations of significant scientific and technical data and information deemed to be of continuing reference value. NASA's counterpart of peer-reviewed formal professional papers but has less stringent limitations on manuscript length and extent of graphic presentations.

- TECHNICAL MEMORANDUM. Scientific and technical findings that are preliminary or of specialized interest, e.g., quick release reports, working papers, and bibliographies that contain minimal annotation. Does not contain extensive analysis.

- CONTRACTOR REPORT. Scientific and technical findings by NASA-sponsored contractors and grantees.

- CONFERENCE PUBLICATION. Collected papers from scientific and technical conferences, symposia, seminars, or other meetings sponsored or cosponsored by NASA.

- SPECIAL PUBLICATION. Scientific, technical, or historical information from NASA programs, projects, and mission, often concerned with subjects having substantial public interest.

- TECHNICAL TRANSLATION. English-language translations of foreign scientific and technical material pertinent to NASA's mission.

Specialized services also include organizing and publishing research results, distributing specialized research announcements and feeds, providing information desk and personal search support, and enabling data exchange services.

For more information about the NASA STI program, see the following:

- Access the NASA STI program home page at http://www.sti.nasa.gov

- Help desk contact information:

https://www.sti.nasa.gov/sti-contact-form/ and select the "General" help request type.

NASA/TM–20230008831

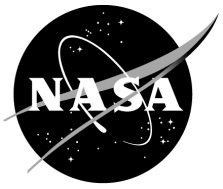

Effects of Strain Rate and Surface Finish on Tensile Properties in High Pressure Hydrogen — A Case Study for LP-DED NASA HR-1

P.S. Chen,[1] M.D. Fullen,[1] M.C. Watwood,[1] B.L Rupp,[1] W.M. Medders,[2] C.C. Katsarelis,[2] and P.R. Gradl[2]

[1]Jacobs ESSCA Group, Huntsville, Alabama
[2]Marshall Space Flight Center, Huntsville, Alabama

National Aeronautics and
Space Administration

Marshall Space Flight Center • Huntsville, Alabama 35812

June 2023

Available from:

NASA STI Information Desk
Mail Stop 148
NASA Langley Research Center
Hampton, VA 23681–2199, USA
757–864–9658

This report is also available in electronic form at
<http://www.sti.nasa.gov>

TABLE OF CONTENTS

1. INTRODUCTION 1

2. PROCEDURES AND METHODS 4

   2.1. Material and LP-DED Process 4
   2.2. Heat Treatment 6
   2.3. Mechanical Testing 6
   2.4. Metallography and SEM Analysis 8

3. RESULTS AND DISCUSSIONS 9

   3.1 Tensile Testing Plan 9
   3.2 Summary of Tensile Properties in Different Environments 10
   3.3 Air and GN_2 Baseline Tensile Tests 13
   3.4 Effects of Hydrogen on Tensile Properties 13
   3.5 Effects of Strain Rate and Surface Finish on HEE Susceptibility 16
   3.6 Hydrogen-Induced Surface Cracking 19
   3.7 Depth of Surface Crack Analysis 22
   3.8 Strain Rate Effect on Hydrogen Diffusion 26
   3.9 Effects of Hydrogen on Fracture Behavior 27
   3.10 Suitability of Slow Strain Rate Tensile Testing for HEE Screening 31
   3.11 Correlation of HEE Screening Test Results and LCF Life in Hydrogen 33

4. RECOMMENDATIONS 34

5. CONCLUSIONS 35

REFERENCES 36

LIST OF FIGURES

1. Material being deposited and observed melt pool using LP-DED. Images used with permissions from: (Left) DM3D Technology and (Right) Formalloy 2

2. (a) An illustration of NASA HR-1 round bar fabrication via LP-DED process, (b) round bars with a length of 4 inches and diameter of 0.6 inches fabricated at a laser power of 1070 watts with virgin powder from lot HRA13 4

3. A SEM image showing NASA HR-1 powder particle morphology 6

4. Geometry and dimensions of the smooth tensile specimen used for testing in 5 ksi gaseous nitrogen and hydrogen environments at ambient temperature. All dimensions are in inches. The specified surface finish (Ra) on the gauge surface is 32 μin or better for specimens to be tested in hydrogen. Two final machining methods, turning and low stress grinding (LSG) were used to produce specimens with two different surface finishes 7

5. The typical microstructure (in x–z plane) of LP-DED NASA HR-1 tensile specimen used for tensile testing in hydrogen. The as-built columnar grain structure has completely recrystallized after heat treatment. The average grain size is approximately 75 μm 9

6. Surface profiles of (a) machined specimen (specimen 210200–124), Ra = 6.7 μin and (b) LSG specimen (specimen 210200–130), Ra = 4.0 μin 12

7. HEE susceptibility comparison for LP-DED NASA HR-1 and the wrought alloy tested at 0.005 in/in/min with two different surface finishes 15

8. Overlaid tensile stress-strain curves for a baseline test in nitrogen and three tests in hydrogen at three different strain rates from 0.005 to 0.0001 in/in/min. The three specimens tested in hydrogen have LSG surface finish 16

9. Effects of strain rate and surface finish on (a) yield stress, (b) ultimate tensile stress, and (c) fracture elongation in hydrogen for LP-DED NASA HR-1. Strain rate appears to have insignificant effects on yield stress and ultimate tensile stress in hydrogen. Both LSG & machined samples exhibit some ductility loss when testing at a strain rate that is slower than 0.0005 in/in/min. Overall, LSG samples performed better than machined samples in hydrogen 18

LIST OF FIGURES (Continued)

10. SEM images showing surface cracking behavior of machined specimens tensile tested in hydrogen at the strain rate of (a) 0.005, (b) 0.0005, and (c) 0.0001 in/in/min. Three images are presented for each sample. Surface cracks became wider and longer when the strain rate is reduced from 0.005 to 0.0005 in/in/min or slower 20

11. SEM images showing surface cracking behavior of LSG specimens tensile tested in hydrogen at the strain rate of (a) 0.005, (b) 0.0005, and (c) 0.0001 in/in/min. Three images are presented for each sample. Surface cracks became wider and longer when the strain rate is reduced from 0.005 to 0.0005 in/in/min or slower 21

12. Optical images showing cross-sectional views of fractured tensile specimens (with machined surface finish) tested in hydrogen at the strain rate of (a) 0.005, (b) 0.0005, and (c) 0.0001 in/in/min. Five images are presented for each sample. Most surface cracks are oriented at approximately 35–45° with respect to the loading direction. The surface cracking mode is predominantly ductile transgranular 24

13. Optical images showing cross-sectional views of fractured tensile specimens (with LSG surface finish) tested in hydrogen at the strain rate of (a) 0.005, (b) 0.0005, and (c) 0.0001 in/in/min. Five images are presented for each sample. Most surface cracks are oriented at approximately 35–45° with respect to the loading direction. The surface cracking mode is predominantly ductile transgranular 25

14. SEM fractography of machined specimens tensile tested in hydrogen at the strain rate of (a) 0.005, (b) 0.0005, and (c) 0.0001 in/in/min. Three images are presented for each sample to show the overall fracture surface, the HEE affected zone near the specimen surface, and hydrogen-induced quasi-cleavage fracture 29

15. SEM fractography of LSG specimens tensile tested in hydrogen at the strain rate of (a) 0.005, (b) 0.0005, and (c) 0.0001 in/in/min. Three images are presented for each sample to show the overall fracture surface, the HEE affected zone near the specimen surface, and hydrogen-induced quasi-cleavage fracture 31

16. (a) HEE susceptibility screening test results obtained at 0.005 in/in/min and (b) the strain-controlled LCF test results at 2% total strain in hydrogen and air for LP-DED NASA HR-1.[13] The trend of HEE screening results by tensile testing correlates well with that of the strain-controlled LCF behavior in hydrogen ... 33

LIST OF TABLES

1. Analyzed chemical composition (wt%) of NASA HR-1 powder (from powder lot HRA13) and its specification 5

2. Correlation between stroke rate and pre-yield strain rate for LP-DED NASA HR-1 8

3. The tensile testing plan intended to investigate the influence of strain rate and surface finish on tensile properties in high pressure hydrogen environment 10

4. Effects of strain rate and surface finish on tensile properties of LP-DED NASA HR-1 at room temperature in air, high pressure gaseous nitrogen and hydrogen environments 11

5. Average room temperature tensile properties of LP-DED NASA HR-1 in air at three strain rates and in 5 ksi inert nitrogen gas at 0.01 in/in/min 13

6. Average room temperature tensile properties, testing duration, and surface roughness for LP-DED NASA HR-1 tested in high pressure hydrogen and inert nitrogen gas environments 14

7. The GH_2/GN_2 ratios of yield stress (YS), ultimate tensile stress (UTS), and ductility (fracture elongation) under three strain rates and two surface finish conditions for LP-DED NASA HR-1 17

8. Effects of strain rate on testing duration, hydrogen diffusion distance, depth of surface cracks, HE category, and fracture driving force. IHE denotes internal hydrogen embrittlement. The depth of surface cracks were measured from the machined specimens at roughly 0.15 inches from the fracture surface and in the vicinity of the specimen shoulder 32

LIST OF ACRONYMS AND SYMBOLS

Al	Aluminum
AM	Additive Manufacturing
ASTM	American Society of Testing and Materials
C	Degree Celsius
Co	Cobalt
Cr	Chromium
D	Diffusivity (Diffusion Coefficient)
DED	Directed Energy Deposition
η phase	Ni_3Ti
F	Degree Fahrenheit
Fe	Iron
GH_2	Gaseous Hydrogen
GHe	Gaseous Helium
GN_2	Gaseous Nitrogen
HE	Hydrogen Embrittlement
HEE	Hydrogen Environment Embrittlement
IHE	Internal Hydrogen Embrittlement
K	Stress Intensity Factor
LCF	Low Cycle Fatigue
LP–DED	Laser Powder Directed Energy Deposition

LIST OF ACRONYMS AND SYMBOLS (Continued)

LRE	Liquid Rocket Engine
LSG	Low Stress Grinding
mm	Millimeter or 0.001 of a Meter
μm	micrometer or 0.000001 of a Meter
MSFC	Marshal Space Flight Center
Mo	Molybdenum
NASA	National Aeronautics and Space Administration
Ni	Nickel
psi	pounds per square inch, an English pressure unit
Ra	arithmetic mean surface roughness
SEM	Scanning Electron Microscopy
Strain Rate	in/in/min (inch/inch/minute)
σ_y	Flow stress at a specific temperature and strain rate
Ti	Titanium
TM	Technical Memorandum
V	Vanadium
W	Tungsten

TECHNICAL MEMORANDUM

EFFECTS OF STRAIN RATE AND SURFACE FINISH ON TENSILE PROPERTIES IN HIGH PRESSURE HYDROGEN — A CASE STUDY FOR LP-DED NASA HR-1

1. INTRODUCTION

Due to exposure to high pressure gaseous hydrogen, mechanical property degradation caused by hydrogen environment embrittlement (HEE) is a critical concern for many materials in liquid hydrogen propulsion systems. Since the early 1980s, the National Aeronautics and Space Administration (NASA) has been performing tensile testing in high pressure hydrogen environments at Marshall Space Flight Center (MSFC) to create a database of candidate materials for propulsion applications. MSFC used to run smooth tensile test at a strain rate of 0.005 in/in/min in high pressure hydrogen environments to evaluate the HEE susceptibility of materials.[1] The tensile test strain rate was changed to 0.0005 in/in/min in recent years based on the recommendation from a published NASA TM.[2] It is well documented that smooth tensile test strain rate influences HEE susceptibility of alloy 718, 4340 steel, 316 stainless steel, and many other alloys.[1,3–7] As a result, the data generated at 0.005 in/in/min and 0.0005 in/in/min showed significant variations in HEE susceptibility for many alloys.

The HEE susceptibility can also be affected by the surface finish condition of a tensile specimen. This is because gaseous hydrogen has a significant influence on microcrack initiation and growth behavior on the specimen surface, particularly when relatively large surface flaws exist on a susceptible material.[2] It has been reported that an increase in the machining rate led to a decline in hydrogen resistance of alloy 718.[8] Surface roughness and defects can act as an embrittling origin and affect the tensile ductility in a high pressure gaseous hydrogen environment.[9] The residual stress of a machined specimen surface can also affect hydrogen embrittlement.[10,11] Per the ASTM standard G142, the method of final machining for specimens to be tested in hydrogen should be by grinding (not turning) to avoid localized grooves and cold worked areas.[12] In this study, the effects of strain rate and specimen surface finish conditions were investigated using smooth tensile tests in 5 ksi high pressure hydrogen environment at NASA-MSFC.

The alloy selected for this investigation was laser powder directed energy deposition (LP-DED) NASA HR-1 (Hydrogen Resistant -1), an AM Fe-Ni-base superalloy that was specifically developed for regenerative rocket engine nozzle applications.[13–16] Optimized materials in the extreme high pressure hydrogen environment for liquid rocket engines and industrial applications remain a key challenge. Additive manufacturing (AM) has provided new design and manufacturing opportunities to reduce cost and schedules, consolidate parts, and optimize performance. The LP-DED process uses concentrated thermal energy, achieved with a laser, to deposit metal by creating a melt pool and injecting or blowing powder into the melt pool, which in turn solidifies, creating a bead.[15] This process allows for freeform fabrication of components or addition of

material to components for the purposes of coating, repair, or modification using local deposition. Freeform components are formed by the precise control of toolpath parameters created from a CAD model that create individual (weld) beads that are deposited to take a final geometric shape. The powder and laser optics are mounted on an integrated deposition head, which allows for the convergence of the laser and powder at a defined focus at the surface of the substrate, where material is melted and cooled to form the bead. The build substrate can be a sacrificial build plate or an existing component. The deposition head is mounted to a robotic arm or gantry system to control the motion through programmed or logic tool paths to deposit material or create features. An example of the process can be seen in Figure 1.

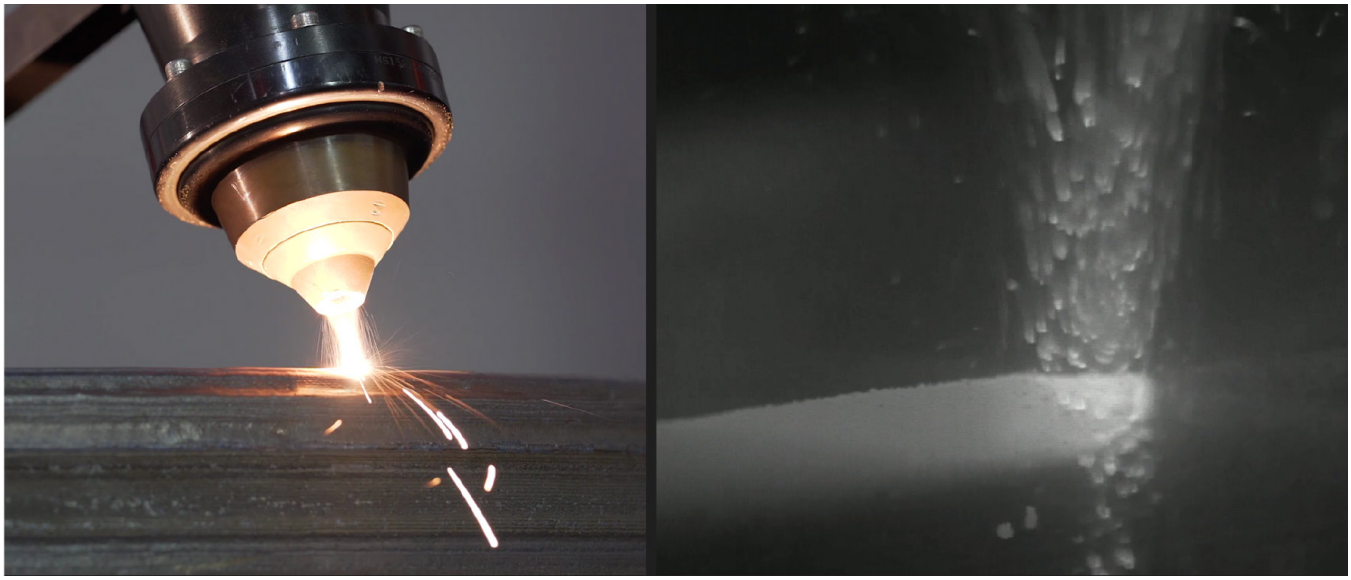

Figure 1. Material being deposited and observed melt pool using LP-DED. Images used with permissions from: (Left) DM3D Technology and (Right) Formalloy.

NASA has advanced NASA HR-1 as a solution for liquid rocket engine components that operate in hydrogen rich environments using various AM techniques.[15,17] The NASA HR-1 for AM applications was specifically formulated for high ductility in high pressure gaseous hydrogen environment in addition to high strength and low cycle fatigue (LCF) resistance. NASA HR-1 meets materials requirements for liquid rocket engine components, including good hydrogen resistance, high conductivity, good LCF performance, and high elongation and strength for components in medium heat flux environments. NASA has completed fabrication of several subscale and full-scale channel wall nozzles in LP-DED NASA HR-1 and completed hot-fire testing.[13,15] This includes refinement of the process to produce thin-walls and various channel geometries to meet the requirements for channel wall nozzle applications.[17–22]

The main objective of this investigation is to better understand the effects of tensile test strain rate and specimen surface finish on the amount of tensile ductility degradation in high pressure gaseous hydrogen environments. Performing smooth tensile tests in high pressure hydrogen

and nitrogen environments can serve as a rapid and economical screening method to determine the relative susceptibility of materials to HEE.[2,23] This paper presents the tensile test results for LP-DED NASA HR-1 in hydrogen and details the material evaluation on the effects of strain rate and surface finish condition on surface cracking behavior and fracture characteristics. The resistance to HEE for LP-DED NASA HR-1 and the wrought alloy is compared under the same testing conditions. Loss of tensile ductility is quantified in terms of changes in elongation at failure in hydrogen to compare HEE susceptibility. The most suitable strain rate and specimen surface finish condition for future HEE screening testing at MSFC are recommended.

2. EXPERIMENTAL PROCEDURES AND METHODS

2.1 Material and LP-DED Process

The material used for this study was multi-pass LP-DED NASA HR-1 round bars deposited on an RPM Innovations (RPMI) machine. The multi-pass LP-DED NASA HR-1 round bar samples were deposited at a laser power of 1070 watts, 16.3 g/min powder feed rate and 40 in/min travel speed. The samples were deposited to a length of 4 inches and 0.6 inches in diameter. An illustration of NASA HR-1 round bar fabrication via LP-DED process is shown in Figure 2(a) and deposited samples in Figure 2(b).

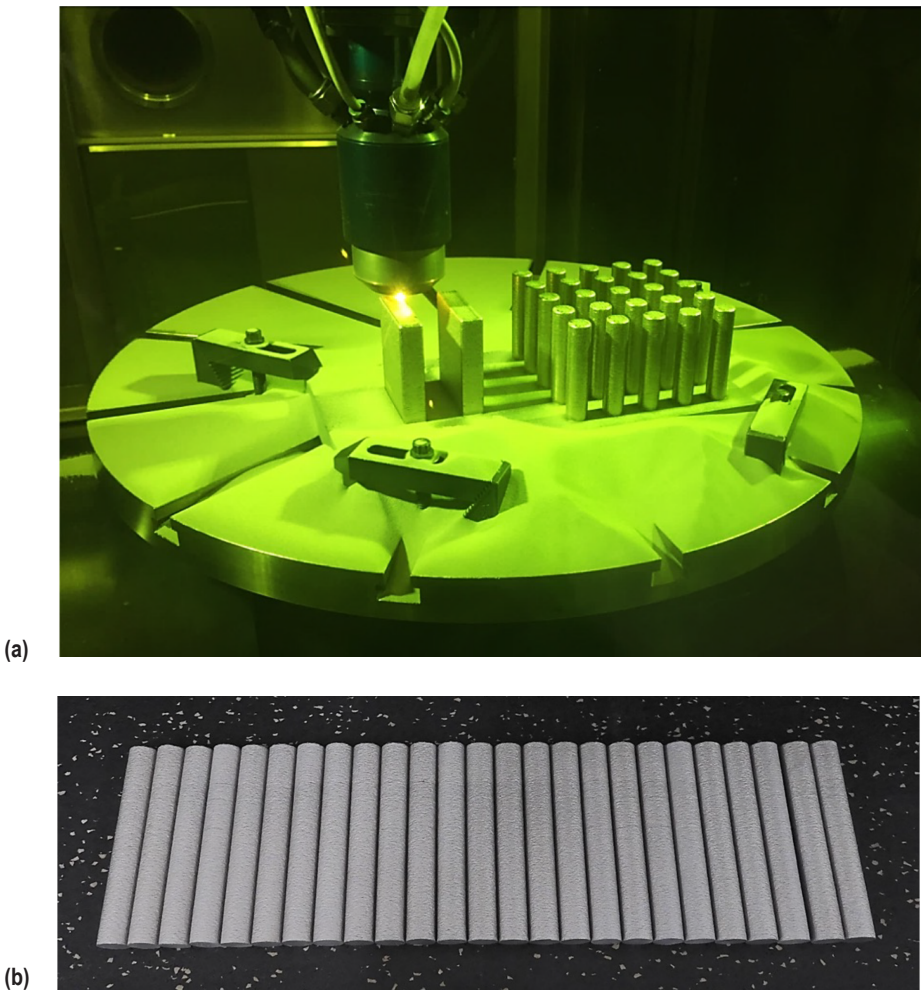

Figure 2. (a) An illustration of NASA HR-1 round bar fabrication via LP-DED process, (b) round bars with a length of 4 inches and diameter of 0.6 inches fabricated at a laser power of 1070 watts with virgin powder from lot HRA13.

The feedstock NASA HR-1 powder used for the LP-DED process was a pre-alloyed rotary-atomized powder produced using a vacuum or by inert induction melting utilizing rotary atomization in argon.[24] The tensile specimens were selected from build numbers 210200-101 to 210200-140. The analyzed chemical composition of the LP-DED NASA HR-1 powder (from powder lot HRA13) and its specification is provided is in Table 1. The powder size distribution was between 45 and 105 μm (–140 mesh/+325 mesh). NASA HR-1 powder is a mostly spherical shape with a few oblong ellipsoidal particles and some traces of satellites. The SEM image showing the typical NASA HR-1 powder morphology for LP-DED process is provided in Figure 3.

Table 1. Analyzed chemical composition (wt%) of NASA HR-1 powder (from powder lot HRA13) and its specification.

Element	Analyzed Composition (wt%)	Specification (wt%)		
		Nominal	Minimum	Maximum
Iron	BAL	BAL	–	–
Nickel	33.90	34.00	33.70	34.30
Chromium	14.45	14.60	14.30	14.90
Cobalt	3.71	3.80	3.60	4.00
Molybdenum	1.83	1.80	1.60	2.00
Tungsten	1.59	1.60	1.40	1.80
Titanium	2.36	2.40	2.20	2.60
Vanadium	0.30	0.30	0.28	0.32
Aluminum	0.24	0.25	0.23	0.27
Sulfur	0.0004	–	–	0.005
Phosphorus	0.0005	–	–	0.005
Carbon	0.0029	–	–	0.03
Silicon	0.017	–	–	0.05
Boron	0.0001	–	–	0.005
Manganese	0.0006	–	–	0.05
Hydrogen	–	–	–	<50 ppm
Oxygen	78 ppm	–	–	<100 ppm (–140/+325 mesh) <200 ppm (–325 mesh/+10 um)
Nitrogen	15 ppm	–	–	<50 ppm

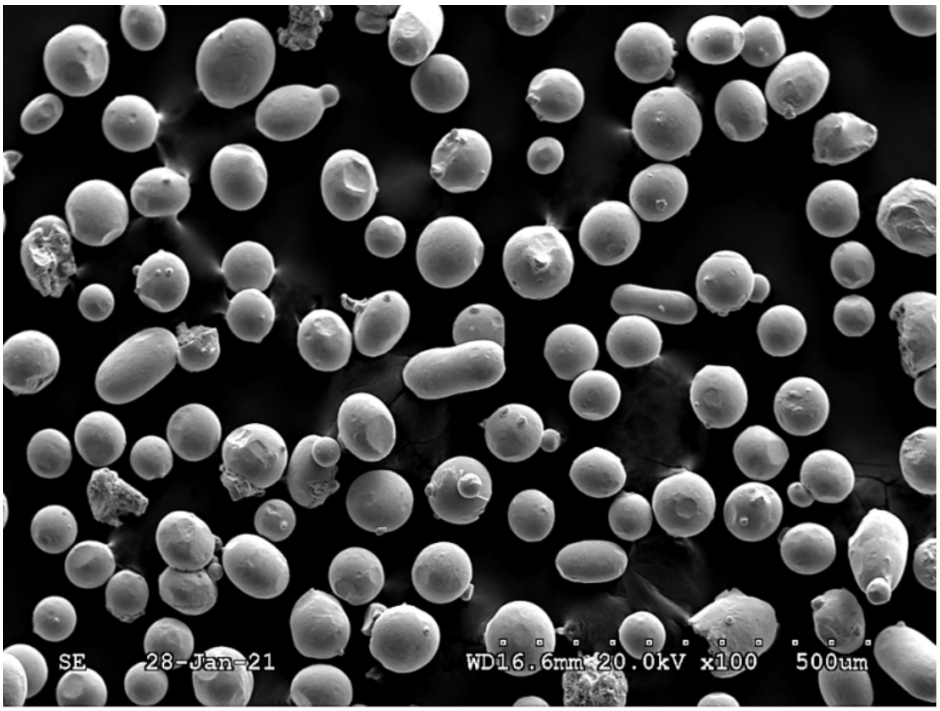

Figure 3. A SEM image showing NASA HR-1 powder particle morphology.

2.2 Heat Treatment

After deposition, the round bar samples require post-processing heat treatment to attain the desirable materials properties. The heat treatment steps include a stress relief, homogenization, solution anneal, and aging treatment. The as-built samples received stress-relief treatment at 1950 °F/1.5h with a slow furnace cool. After stress relief, the samples were subjected to a homogenization treatment at 2125 °F/6h in a vacuum furnace. At the end of homogenization treatment, the samples were argon quenched to minimize η-phase precipitation. Then, the samples were solution annealed at 1950 °F/1h in vacuum with an argon quench, followed by a 2-step aging at 1275 °F/16h + 1150 °F/16h (total 32 hours) in a vacuum furnace to complete the heat treatment process.[13]

2.3 Mechanical Testing

All tensile tests were conducted at the NASA-MSFC Hydrogen Test Facility (HTF). Tensile testing in 5 ksi gaseous nitrogen and hydrogen environments was conducted in Test Cell 23 (TC-23) in Building 4628 at MSFC. The smooth tensile sample had a uniform gage, 0.25 inch in diameter by 1.25 inch in length. The first part of this study examined the effects of tensile test strain rate on HEE susceptibility. A series of baseline tests were run in ambient air over a range of strain rates to investigate the influence of strain rate on tensile properties of LP-DED NASA HR-1. Smooth tensile testing was also performed at room temperature in a gaseous nitrogen (GN_2) environment at a pressure of 5 ksi to see the effect of inert gas pressure on tensile properties. Smooth tensile testing was then performed at three different strain rates in gaseous hydrogen environment

to see the effects of strain rate on HEE susceptibility. The second part of this study consisted of studying the effects of different machining methods on HEE susceptibility. The specified surface finish (Ra, value of arithmetic mean surface roughness) for the gauge section was 32 µin or better per ASTM standard G142. Final machining of the gauge section was performed by either turning or low stress grinding to compare the effects of specimen surface conditions on HEE susceptibility. The surface roughness of the specimens tested in high pressure gas environments was measured with a contact profilometer to determine the arithmetic average roughness noted as Ra, which is the absolute average relative to the base length. Shape and dimension of the smooth tensile specimen used for testing at ambient temperature in 5 ksi gaseous nitrogen and hydrogen environments is shown in Figure 4.

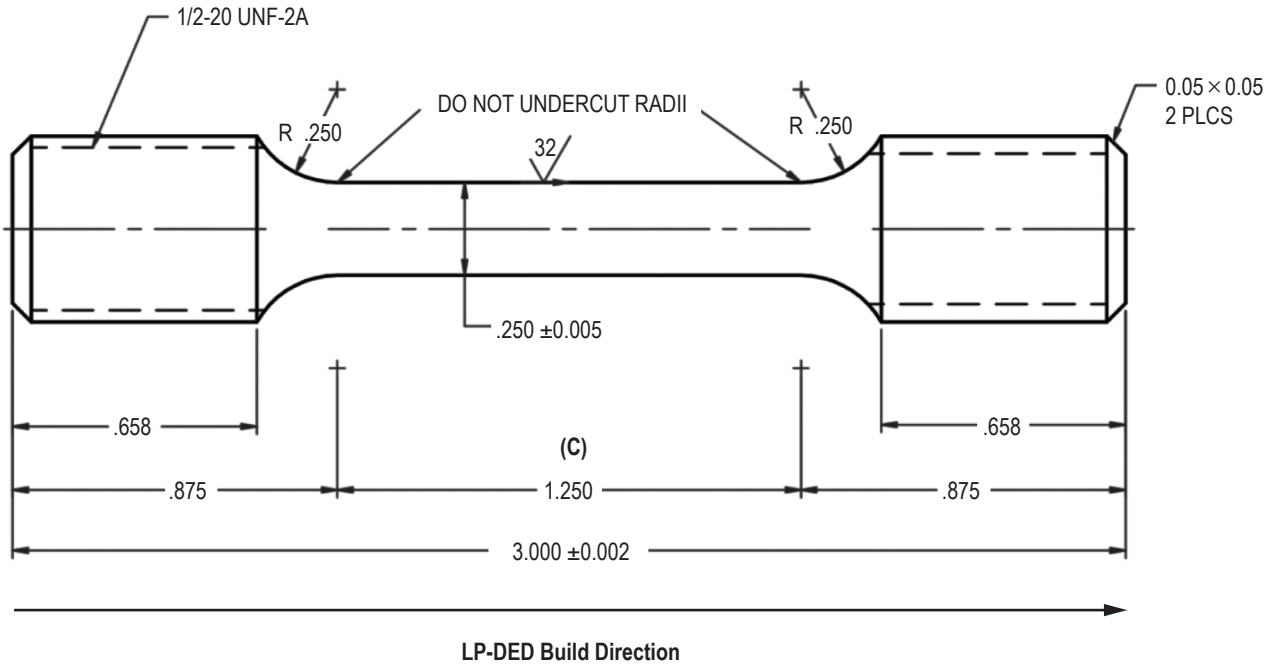

Figure 4. Geometry and dimensions of the smooth tensile specimen used for testing in 5 ksi gaseous nitrogen and hydrogen environments at ambient temperature. All dimensions are in inches. The specified surface finish (Ra) on the gauge surface is 32 µin or better for specimens to be tested in hydrogen. Two final machining methods, turning and low stress grinding (LSG) were used to produce specimens with two different surface finishes.

Stroke control is the traditional means of running tensile tests in hydrogen.[1] The historic standard rate for smooth tensile testing in hydrogen is the stroke rate that results in a pre-yield strain rate of 0.005 in/in/minute.[1] In this study, smooth tensile tests were run in a gaseous hydrogen (GH_2) environment in a stroke control manner that generated three different pre-yield strain rates, 0.005 in/in/min, 0.0005 in/in/min, and 0.0001 in/in/min. A +/- 1-inch Linear Variable Differential Transducer (LVDT) was used for displacement feedback. Stress measurements were derived from a load cell calibrated to 20,000 pounds and specimen dimension measurements.

Strain measurements were derived from a 1.00-inch extensometer calibrated to 15% strain. After 15% strain was achieved during the test, stroke data was used to calculate strain. It must be noted that the actual stroke rate needed to obtain the desirable pre-yield strain rate depends on the test machine, the specimen design, and the alloy tested.[1] The correlation between stroke rate and strain rate (pre-yield) for LP-DED NASA HR-1 is shown in Table 2. The slower strain rate tests were intended to closely characterize the effects of strain rate on hydrogen embrittlement susceptibility, which generally increases with decreasing strain rates. Fracture elongation was obtained based on the change in the total length of the specimen punch marks (1 inch gauge marks) before and after the test. HEE susceptibility was evaluated by relative fracture elongation, which is a ratio of fracture elongation under high pressure gaseous hydrogen (GH_2) to that in high pressure inert gaseous nitrogen (GN_2).[2]

Table 2. Correlation between stroke rate and pre-yield strain rate for LP-DED NASA HR-1.

Material	Type of test	Media	Pressure (psi)	Stroke rate (in/min)	*Strain rate (in/in/min)
LP–DED NASA HR–1	Smooth Tensile	GN_2	5000	0.05	0.01
		GH_2	5000	0.028	0.005
				0.0008	0.0005
				0.0005	0.0001

* Denotes pre-yield strain rate

2.4 Metallography and SEM Analysis

Selected broken tensile specimens were metallurgically characterized. Metallographic samples were prepared by sectioning through the gage section along the tensile loading direction (build direction) to determine the depth of surface cracks and observe the surrounding microstructure. Chemical etching was conducted with waterless Kaling's reagent immersed for 2–3 minutes. Surface cracking behavior was analyzed by the use of a Hitachi scanning electron microscope (SEM). Fracture surfaces of representative specimens were also analyzed with the Hitachi SEM to explore the effects of hydrogen on tensile fracture behavior. Optical microscopy was performed with a Leica microscope to observe the depth of surface cracks and deformation-induced microstructure near the fracture surface.

3. RESULT AND DISCUSSIONS

The typical microstructure of LP-DED NASA HR-1 tensile sample (in x–z plane) with the full heat treatment is shown in Figure 5. The micrograph was taken near the threaded end of a tensile sample where plastic deformation was negligible. A high degree of recrystallization had taken place after heat treatment, and the average grain size is ~75 μm. The grain boundaries are very clean as the undesirable grain-boundary η phase (Ni_3Ti) is reduced to a very low level after heat treatment.

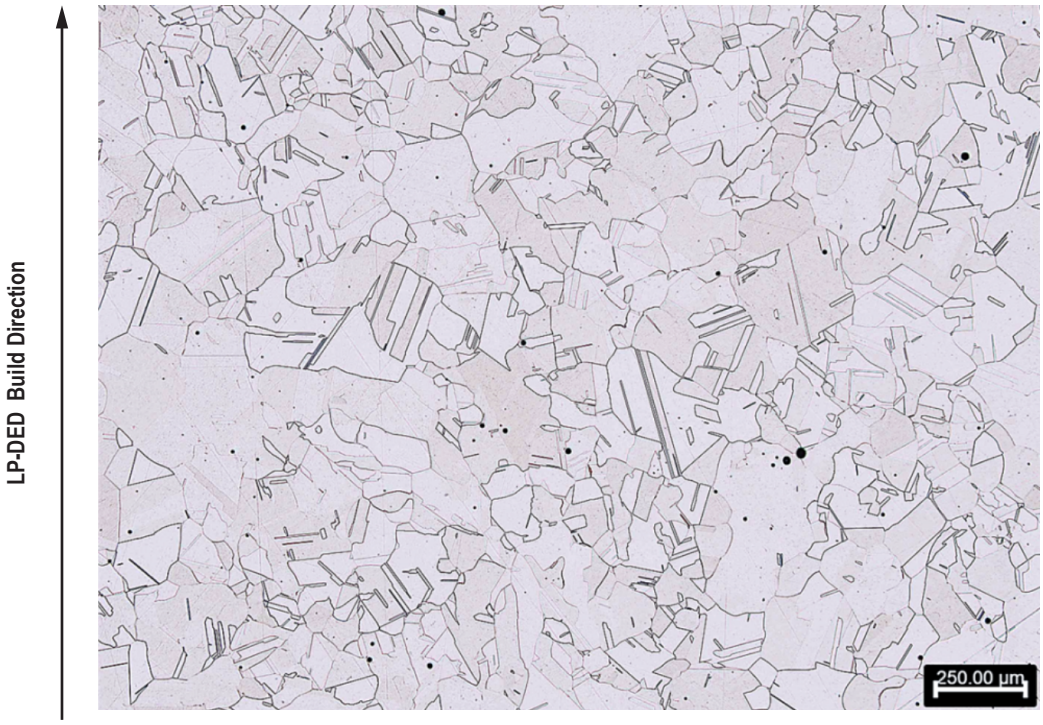

Figure 5. The typical microstructure (in x–z plane) of LP-DED NASA HR-1 tensile specimen used for tensile testing in hydrogen. The as-built columnar grain structure has completely recrystallized after heat treatment. The average grain size is approximately 75 μm.

3.1 Tensile Testing Plan

Table 3 shows the tensile testing plan that is intended to investigate the influence of strain rate and surface finish condition on tensile properties in hydrogen at room temperature. A series of baseline tensile tests were run in ambient air at three strain rates to investigate the effects of test speed on tensile properties without the influence of hydrogen. Static gas pressure is a parameter

that can influence the mechanical response of solids.[25] Therefore, tensile tests were also performed in an inert gaseous nitrogen environment at a strain rate of 0.01 in/in/min to provide additional baseline tensile data. To evaluate the susceptibility of HEE, tensile testing was conducted in 5ksi gaseous hydrogen environment at room temperature under three different strain rates, 0.005 in/in/min, 0.0005 in/in/min, and 0.0001 in/in/min. HEE effects are a function of temperature and maximum HEE susceptibility usually occurs at near room temperature.[2] Effects of specimen surface finish condition on HEE were also investigated. Some specimens have machined surface finish (by turning), while the others have a low stress grind surface finish. To determine the level of variability that can be expected when testing in hydrogen, repeat tests (3–4 specimens) were performed in hydrogen.

Table 3. The tensile testing plan intended to investigate the influence of strain rate and surface finish on tensile properties in high pressure hydrogen environment.

		Testing Environment			
		Ambient air	5ksi GN_2, Room Temperature	5ksi GH_2 Room Temperature	5ksi GH_2, Room Temperature
Type of Test	Strain Rate	# of Specimen	# of Specimen	# of Specimen (Machined, Ra <32 µin)	# of Specimen (LSG, Ra <32 µin)
Smooth Tensile	0.01 in/in/min	3	3		
	0.001 in/in/min	3			
	0.0005 in/in/min	3			
	0.005 in/in/min			4	4
	0.0005 in/in/min			4	4
	0.0001 in/in/min			2	3

3.2 Summary of Tensile Properties in Different Environments

The influence of strain rate and surface finish on tensile properties at room temperature in air and high pressure gaseous nitrogen and gaseous hydrogen environments is presented in Table 4. The typical values of arithmetic mean surface roughness, Ra, for the specimen tested in hydrogen were measured with a contact profilometer and the results are given in Table 4. All specimens for tensile testing in hydrogen meet the minimum surface roughness (see Figure 4) requirement of 32 µin or better, which conforms to ASTM standard G-142.[12] Overall, the surface roughness of LSG specimens is slightly smoother than that of the machined specimens. Representative surface profiles of a machined (Ra = 6.7 µin) and a LSG (Ra = 4.0 µin) specimen are illustrated in Figure 6. As shown, there is the presence of a regular fluctuating profile (waviness from the surface texture) in both machined and LSG samples. The maximum profile height is around 0.8 µm for the machined sample (Figure 6(a)), which is slightly larger than that of the LSG sample. The LSG sample has a slightly smoother surface, and the maximum profile height is approximately 0.5 µm (Figure 6(b)).

Table 4. Effects of strain rate and surface finish on tensile properties of LP-DED NASA HR-1 at room temperature in air, high pressure gaseous nitrogen and hydrogen environments.

ID #.	Media	Pressure (psi)	Strain Rate	Surface Finish	Surface Roughness, Ra (µin)	YS (ksi)	UTS (ksi)	%EL
210200–102	Air	ambient	0.01 in/in/min	Machined	–	77.44	152.63	40.50
210200–103	Air	ambient	0.01 in/in/min	Machined	–	77.29	152.60	41.22
210200–104	Air	ambient	0.01 in/in/min	Machined	–	76.58	151.55	40.80
210200–105	Air	ambient	0.001 in/in/min	Machined	–	78.59	153.81	40.75
210200–106	Air	ambient	0.001 in/in/min	Machined	–	77.12	152.12	41.96
210200–131	Air	ambient	0.001 in/in/min	Machined	–	77.42	152.98	40.92
210200–108	Air	ambient	0.0005 in/in/min	Machined	–	76.36	151.76	41.49
210200–109	Air	ambient	0.0005 in/in/min	Machined	–	77.40	152.44	41.01
210200–113	Air	ambient	0.0005 in/in/min	Machined	–	77.72	152.81	40.28
210200–114	GN_2	5000	0.01 in/in/min	Machined	–	77.17	152.83	41.13
210200–115	GN_2	5000	0.01 in/in/min	Machined	–	76.43	153.10	40.70
210200–117	GN_2	5000	0.01 in/in/min	Machined	–	75.99	152.84	39.80
210200–119	GH_2	5000	0.005 in/in/min	Machined	25.2	76.63	150.70	38.52
210200–120	GH_2	5000	0.005 in/in/min	Machined	7.2	76.66	151.44	38.82
210200–122	GH_2	5000	0.005 in/in/min	Machined	18.6	78.02	153.79	38.39
210200–123	GH_2	5000	0.0005 in/in/min	Machined	7.3	75.93	147.36	32.84
210200–124	GH_2	5000	0.0005 in/in/min	Machined	6.7	76.17	148.90	33.00
210200–126	GH_2	5000	0.0005 in/in/min	Machined	9.9	77.72	150.36	31.24
210200–127	GH_2	5000	0.0005 in/in/min	Machined	3.2	75.85	149.54	32.34
210200–128	GH_2	5000	0.0001 in/in/min	Machined	6.7	75.89	146.87	35.69
210200–129	GH_2	5000	0.0001 in/in/min	Machined	8.6	77.87	147.07	30.88
210200–110	GH_2	5000	0.005 in/in/min	LSG	4.4	75.13	152.93	42.06
210200–111	GH_2	5000	0.005 in/in/min	LSG	5.4	76.22	154.51	42.46
210200–112	GH_2	5000	0.005 in/in/min	LSG	3.8	76.59	154.96	41.88
210200–116	GH_2	5000	0.005 in/in/min	LSG	3.3	76.16	154.97	40.02
210200–118	GH_2	5000	0.0005 in/in/min	LSG	4.3	78.11	154.01	35.11
210200–130	GH_2	5000	0.0005 in/in/min	LSG	4.0	74.62	150.36	33.83
210200–137	GH_2	5000	0.0005 in/in/min	LSG	3.9	74.69	148.73	35.18
210200–139	GH_2	5000	0.0001 in/in/min	LSG	3.9	74.45	148.86	35.12
210200–101	GH_2	5000	0.0001 in/in/min	LSG	4.4	75.76	150.60	36.23

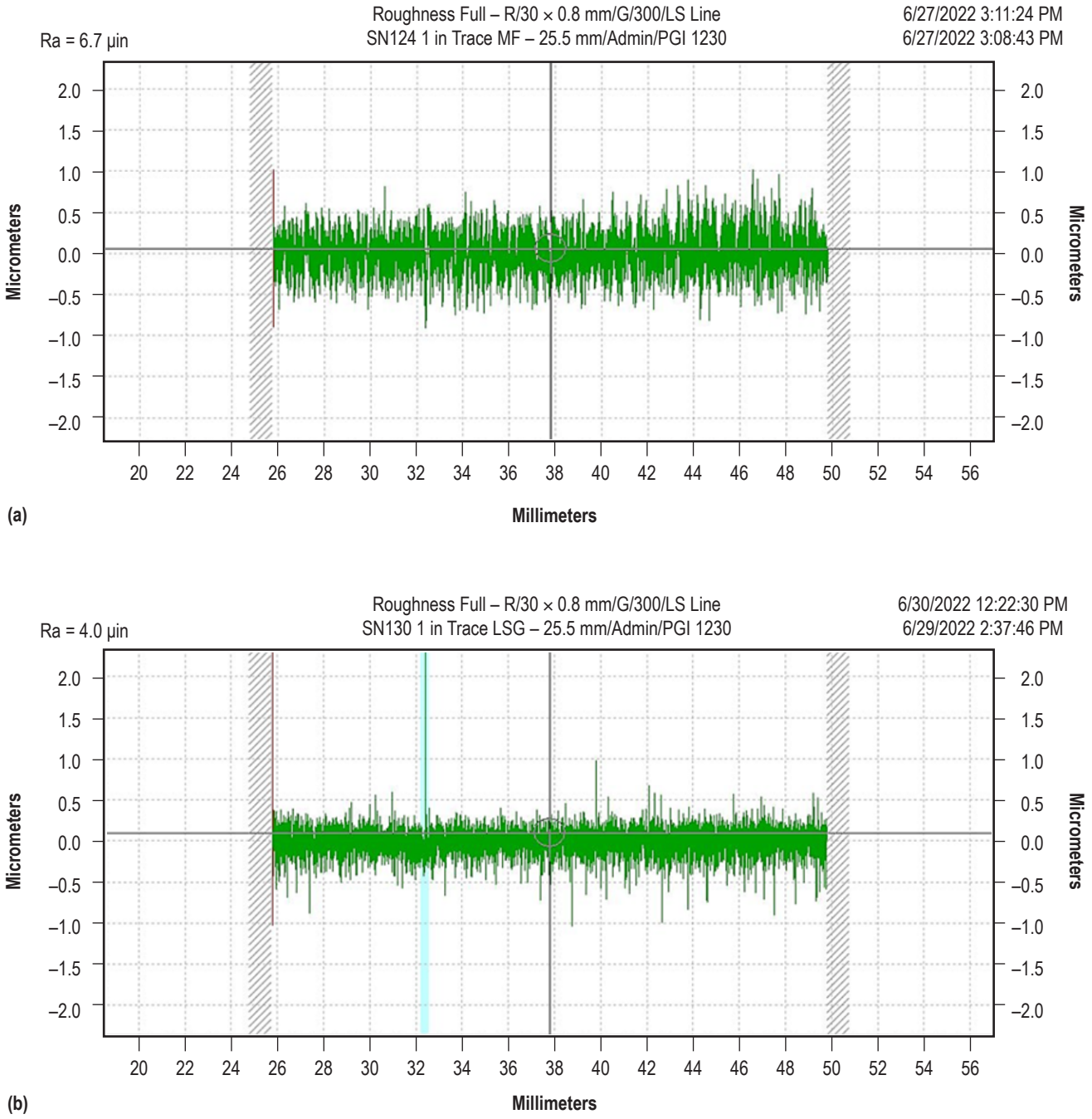

Figure 6. Surface profiles of (a) machined specimen (specimen 210200–124), Ra = 6.7 µin and (b) LSG specimen (specimen 210200–130), Ra = 4.0 µin.

3.3 Air and GN_2 Baseline Tensile Tests

The baseline test results in air and an inert gaseous nitrogen environment are summarized in Table 5. As shown, tensile test strain rate, in the range of 0.01 in/in/min to 0.0005 in/in/min, has no effect on tensile properties in ambient air. It was also found that the 5 ksi gaseous nitrogen pressure has negligible effects on tensile properties for LP-DED NASA HR-1. Metal bonds tend to strengthen when they become shorter under very high pressure that is close to the elastic modulus of the material.[25] The 5 ksi gaseous nitrogen pressure is significantly lower than the elastic modulus of LP-DED NASA HR-1 that is around 30 Msi. This explains why the 5 ksi nitrogen gas pressure has no noticeable effect on tensile properties, as the pressure is too low to compress crystal structure and strengthen the metal bonds. This finding agrees well with a prior study that hydrostatic pressure below 218 ksi (1500 Mpa) has a relatively minor effect on the YS, UTS, and ductility of most ductile metals.[26]

Table 5. Average room temperature tensile properties of LP-DED NASA HR-1 in air at three strain rates and in 5 ksi inert nitrogen gas at 0.01 in/in/min.

Material	Media	Pressure (psi)	Strain Rate	Testing Duration (min)	Surface Finish	YS (ksi)	UTS (ksi)	%EL
LP–DED NASA HR–1	Air	ambient	0.01 in/in/min	~ 10	Machined	77.10	152.26	40.84
	Air	ambient	0.001 in/in/min	25 – 35	Machined	77.71	152.97	41.21
	Air	ambient	0.0005 in/in/min	500 – 600	Machined	77.16	152.34	40.93
	GN_2	5000	0.01 in/in/min	~ 10	Machined	76.53	152.92	40.54

3.4 Effects of Hydrogen on Tensile Properties

The average tensile properties for LP-DED NASA HR-1 and the wrought alloy tested in 5 ksi inert gas (nitrogen and helium) and hydrogen environments are given in Table 6. It must be noted that the reduction in strain rate increases the exposure time in hydrogen significantly from approximately 25–35 minutes (at 0.005 in/in/min) to roughly 800–900 minutes (at 0.0001 in/in/min). LP-DED NASA HR-1 has lower strength but is significantly more ductile than the wrought alloy in hydrogen. Strength reduction is part of the trade to obtain an optimal balance of five key material properties when using AM.[13] The five key material properties for LRE applications are as follows:

(1) Mechanical strength
(2) Ductility
(3) Low cycle fatigue (LCF)
(4) Hydrogen environment embrittlement (HEE)
(5) Thermal conductivity

These five key properties are all interrelated and were taken into consideration when optimizing the formulation and heat treatment for LP-DED NASA HR-1. A moderate strength reduction improves ductility and LCF life significantly, which is important for low-cycle fatigue critical components such as the LRE nozzles.[13]

Table 6. Average room temperature tensile properties, testing duration, and surface roughness for LP-DED NASA HR-1 tested in high pressure hydrogen and inert nitrogen gas environments.

Material	Media	Pressure (psi)	Strain Rate	Testing Duration (min)	Surface Finish	Roughness, Ra (µin)	YS (ksi)	UTS (ksi)	%EL
LP–DED NASA HR–1	GN_2	5000	0.01 in/in/min	~ 10	Machined	–	76.53	152.92	40.54
	GH_2	5000	0.005 in/in/min	25 – 35	Machined	17.0	77.10	151.98	38.58
	GH_2	5000	0.0005 in/in/min	500 – 600	Machined	6.8	76.42	149.04	32.36
	GH_2	5000	0.0001 in/in/min	800 – 900	Machined	7.6	76.88	146.97	33.29
	GH_2	5000	0.005 in/in/min	25 – 35	LSG	4.2	76.03	154.34	41.61
	GH_2	5000	0.0005 in/in/min	500 – 600	LSG	4.1	75.81	151.03	34.71
	GH_2	5000	0.0001 in/in/min	800 – 900	LSG	4.1	75.11	149.73	35.68
Wrought NASA HR–1	GHe	5000	0.01 in/in/min	~10	Machined	< 32	136.93	183.07	23.57
	GH_2	5000	0.005 in/in/min	30 – 40	Machined		128.83	175.37	23.40

Hydrogen has an insignificant effect on tensile properties for LP-DED NASA HR-1 and the wrought alloy when tested at the strain rate of 0.005 in/in/min as shown in Table 6. HEE susceptibility comparison for LP-DED NASA HR-1 and the wrought alloy tested at 0.005 in/in/min is presented in Figure 7. LP-DED NASA HR-1 with LSG surface finish has no ductility loss in hydrogen, and its ductility (41.61%) is significantly higher than that of the wrought alloy (23.4%) by approximately 18%. The machined samples exhibit a slight 2% ductility loss (38.4 %) in hydrogen at the same strain rate. There is noticeable tensile ductility reduction in hydrogen at slower strain rates of 0.0005 in/in/min and 0.0001 in/in/min. The machined specimens have slightly more ductility degradation than the LSG specimens in hydrogen. At the strain rate of 0.0005 in/in/min rate, fracture elongation for the specimens with LSG and machined surface finish decreases to 34.71% and 32.36%, respectively. It is interesting to note that there is no further ductility reduction when the strain rate was reduced from 0.0005 to 0.0001 in/in/min. Although LP-DED NASA HR-1 exhibits some ductility loss after tensile testing at very slow strain rate for 9–14 hours in hydrogen, its tensile ductility remains higher than 33–35%, which is significantly more ductile than any γ′-strengthened superalloys in hydrogen.

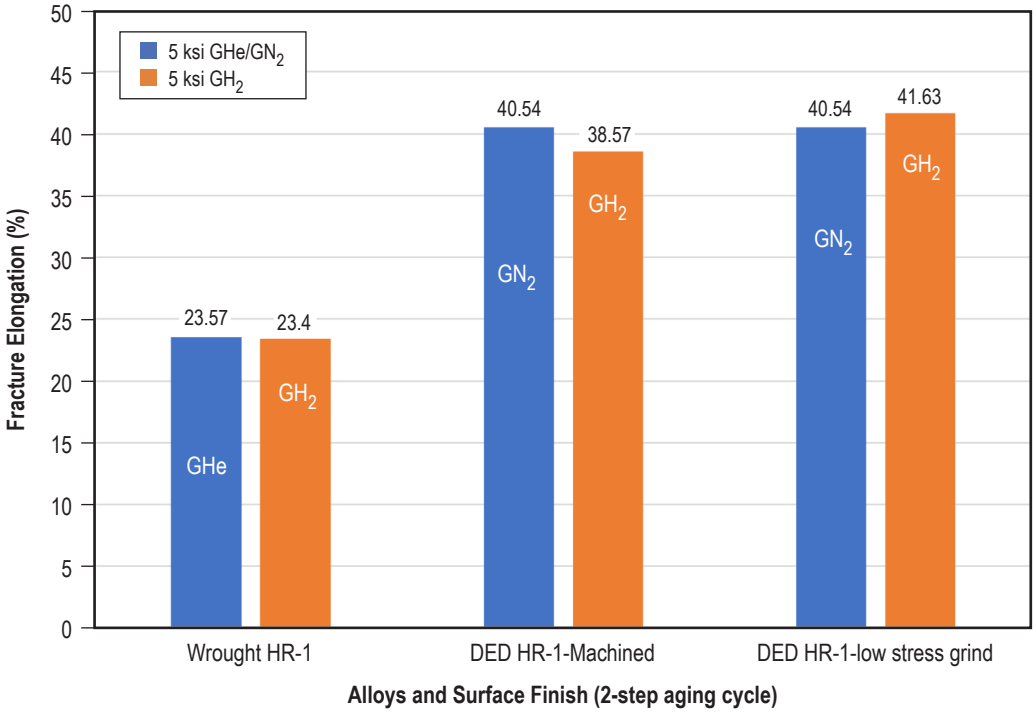

Figure 7. HEE susceptibility comparison for LP-DED NASA HR-1 and the wrought alloy tested at 0.005 in/in/min with two different surface finishes.

Representative tensile stress-strain curves from a baseline test in nitrogen and three tests in hydrogen at three different strain rates are shown in Figure 8. The three specimens tested in hydrogen have LSG surface finish. It must be noted that the fracture elongation values shown on the stress-strain curves are in the range of 39–46%, approximately 4–5% higher than those obtained from the change in the total length of the specimen punch marks (1 inch gauge marks) before and after the test. This discrepancy occurs because the 1.00-inch extensometer was calibrated to 15% strain, and strain values after 15% strain were derived from the stroke data. Serrated stress-strain behavior was found for the specimen tested at 0.005 in/in/min in hydrogen due to the Portevin-Le Chatelier (PLC) effect.[13] Tensile testing in hydrogen can trigger the PLC effect, and the serrated stress-strain flow behavior is caused by the dragging effect of hydrogen atoms on dislocations. All specimens tested in hydrogen display similar strain hardening behavior before reaching the UTS. As shown in Figure 8, the influence of hydrogen on tensile behavior is negligible when tested at the standard strain rate of 0.005 in/in/min. The effects of hydrogen on tensile behavior became more noticeable with decreases in strain rate to 0.0005 and 0.0001 in/in/min. LP-DED NASA HR-1 remains very ductile after lengthy tensile testing in hydrogen, as evidenced by the gradual development of tensile fracture. There is still 4–6% ductility (fracture elongation) between the onset of necking and final fracture.

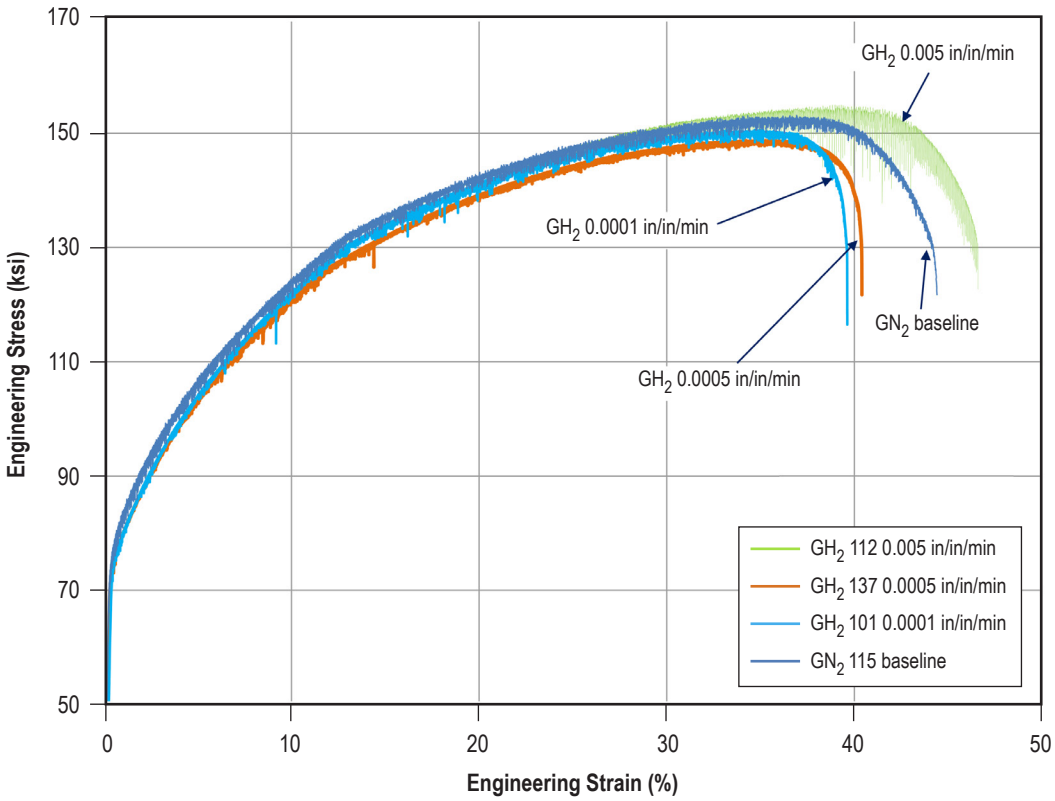

Figure 8. Overlaid tensile stress-strain curves for a baseline test in nitrogen and three tests in hydrogen at three different strain rates from 0.005 to 0.0001 in/in/min. The three specimens tested in hydrogen have LSG surface finish.

3.5 Effects of Strain Rate and Surface Finish on HEE Susceptibility

Table 7 shows the ratios of yield stress (YS), ultimate tensile stress (UTS), and ductility (fracture elongation) for LP-DED and wrought NASA HR-1 tested in hydrogen as compared to that in inert gas environments (GH_2/GHe or GH_2/GN_2). Compared with the wrought alloy, LP-DED NASA HR-1 exhibits a similar GH_2/GN_2 ductility ratio (1.03 and 0.95 for LSG and machined surface finish, respectively) to that of the wrought alloy (0.99) at the strain rate of 0.005 in/in/min. However, LP-DED NASA HR-1 exhibits slightly higher YS and UTS ratios (0.99–1.01) than the wrought alloy (0.94–0.96). Hydrogen embrittlement susceptibility can be affected by the stress imposed on cracks during plastic deformation, which depends on the strength and strain hardening rate of the alloys.[3] Wrought NASA HR-1 has higher strength but lower strain hardening capability than the LP-DED alloy, which can explain the discrepancy in the YS and UTS ratios between them.[13] There is larger force driving crack propagation for alloys with higher strengths due to the increase in the stress intensity at the cracks, which is material strength dependent.

Plots that summarize the effects of strain rate and surface finish on tensile properties in hydrogen for LP-DED NASA HR-1 are presented in Figure 9. The baseline tensile data (in ambient air and nitrogen) is also given in the plots to compare tensile properties under the influence of

hydrogen. Both LSG & machined samples exhibit a negligible reduction in yield stress (1–2 ksi) in hydrogen regardless of the strain rate, which indicates that hydrogen had little effect on the stress required to initiate plastic deformation (see Figure 9(a)). Ultimate tensile stress (UTS) appears to be slightly influenced by hydrogen at slower strain rates as shown in Figure 9(b). Both LSG & machined samples exhibit no reduction in UTS at 0.005 in/in/min in hydrogen. Tensile testing at a strain rate that is slower than 0.0005 in/in/min led to a slight reduction in UTS (3 – 8 ksi). The machined samples exhibit slightly lower UTS (~3 ksi) than the LSG samples at all three strain rates. Despite the slight reduction in UTS, the UTS ratios (GH_2/GN_2) for all conditions are above 0.96 (> 96%), indicating that hydrogen has insignificant effect on UTS for LP-DED NASA HR-1.

Table 7. The GH_2/GN_2 ratios of yield stress (YS), ultimate tensile stress (UTS), and ductility (fracture elongation) under three strain rates and two surface finish conditions for LP-DED NASA HR-1.

Material	Media	Pressure (psi)	Strain Rate	Testing Duration (min)	Surface Finish	Roughness, Ra (µin)	YS Ratio (GH_2/GN_2)	UTS Ratio (GH_2/GN_2)	Ductility Ratio (GH_2/GN_2)
LP–DED NASA HR–1	GH_2	5000	0.005 in/in/min	25–35	Machined	17.0	1.01	0.99	0.95
			0.0005 in/in/min	500 – 600		6.8	1.00	0.97	0.80
			0.0001 in/in/min	800 – 900		7.6	1.00	0.96	0.82
			0.005 in/in/min	25 – 35	LSG	4.2	0.99	1.01	1.03
			0.0005 in/in/min	500 – 600		4.1	0.99	0.99	0.86
			0.0001 in/in/min	800 – 900		4.1	0.98	0.98	0.88
Wrought NASA HR–1	GH_2	5000	0.005 in/in/min	30 – 40	Machined	< 32	0.94	0.96	0.99

The primary effect of hydrogen is on plastic deformation and ductility. Figure 9(c) shows the relationship between fracture elongation, strain rate, surface finish condition, and testing environments for LP-DED NASA HR-1. Tensile elongation ratio in hydrogen vs. helium or nitrogen (GH_2/GHe or GH_2/GN_2) is often used to assess HEE susceptibility.[2] As can be seen, the final machining method on smooth tensile specimens has an influence on HEE susceptibility. An apparent trend is that the LSG specimens have slightly higher tensile ductility than the machined specimens in hydrogen at all three strain rates. As shown in Figure 9(c), the GH_2/GN_2 fracture elongation ratio varies from 95–103% when tested at 0.005 in/in/min. The machined samples exhibit a slight reduction in fracture elongation from 40.54% in nitrogen to 38.58% in hydrogen. The LSG samples show no signs of ductility loss during smooth tensile testing at the same strain rate in hydrogen. Both LSG & machined samples exhibit some ductility loss when testing at a strain rate that is slower than 0.0005 in/in/min. It is interesting to note that a further decrease in strain rate from 0.0005 to 0.0001 in/in/min does not lead to further degradation in tensile ductility. The reduction in fracture elongation at slower strain rates is likely associated with crack growth assisted tensile fracture during lengthy tensile testing in hydrogen, which will be discussed in sections 3.6 (Hydrogen-Induced Surface Cracking) and 3.10 (Suitability of Slow Strain Rate Tensile Testing for HEE Screening). Extensive crack growth can lead to premature failure before reaching the expected tensile ductility level.

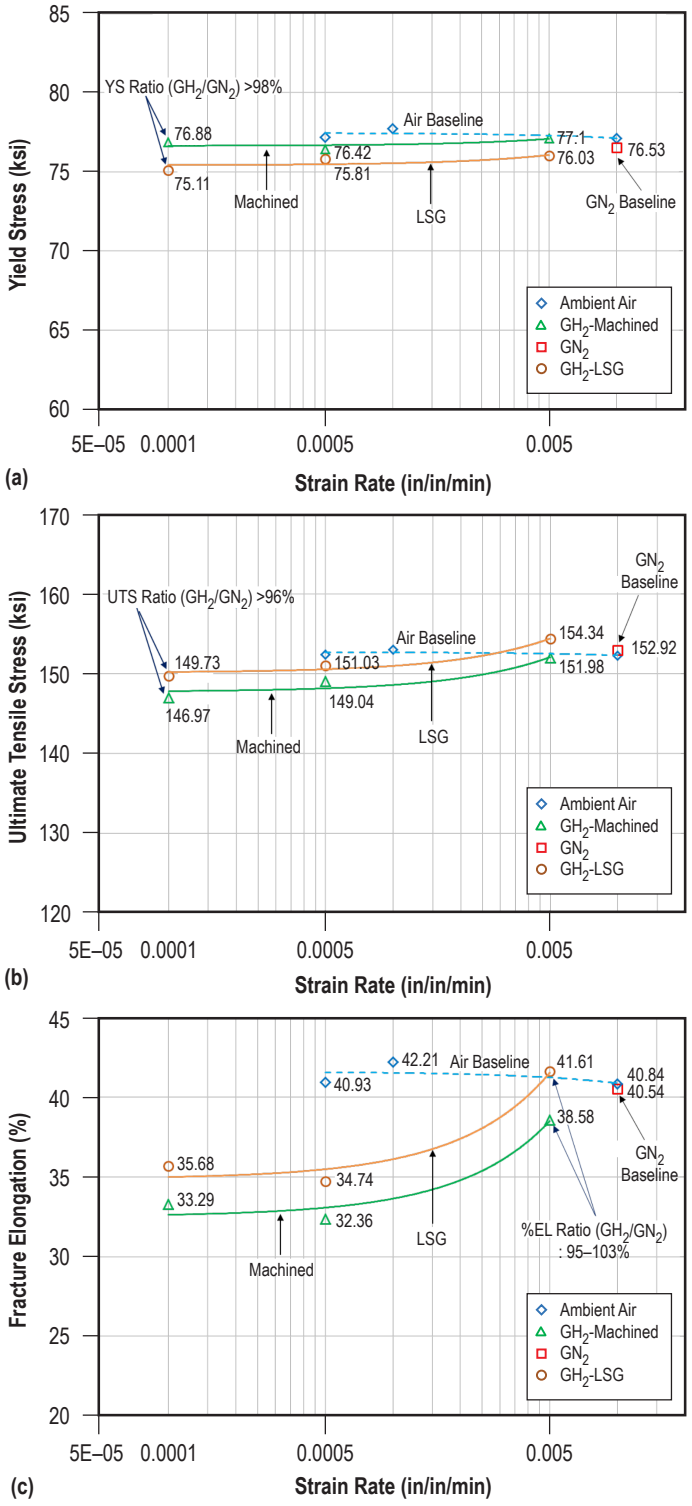

Figure 9. Effects of strain rate and surface finish on (a) yield stress, (b) ultimate tensile stress, and (c) fracture elongation in hydrogen for LP-DED NASA HR-1. Strain rate appears to have insignificant effects on yield stress and ultimate tensile stress in hydrogen. Both LSG & machined samples exhibit some ductility loss when testing at a strain rate that is slower than 0.0005 in/in/min. Overall, LSG samples performed better than machined samples in hydrogen.

3.6 Hydrogen-Induced Surface Cracking

The deformed tensile specimen surfaces were examined using SEM to analyze the hydrogen-induced surface cracking behavior. Figures 10 and 11 present the specimen surface characteristics comparison between machined and LSG specimens after tensile testing in hydrogen under three strain rates. Signs of necking can be seen in all specimens, but the specimens tested at 0.005 in/in/min exhibit more distinct localized necking and shear lips than that tested at slower strain rates. The machined specimen surface is slightly rougher than the LSG specimen surface after tensile testing in hydrogen. There are a series of visible fine machining traces on the machined specimen surface due to the turning process as shown in Figure 10(a) and (b). Both machined and LSG specimens have many small surface cracks after tensile testing in hydrogen at 0.005 in/in/min. The machined specimens have more pronounced surface cracks than the LSG specimens. The surface cracks on the LSG specimen are very shallow and randomly orientated. Some surface cracks on the machined specimens were generated along the machining traces and are perpendicular to the tensile loading direction as shown in Figure 10(a). It is evident that surface crack formation can be assisted by the machining marks that act as the embrittling origin of HEE and affect tensile properties.

The propensity of surface cracking increased with decreasing strain rate. Both machined and LSG specimens exhibit more surface cracks after tensile testing at 0.0005 in/in/min or slower in hydrogen. As can be seen in Figures 10(b) and 11(b), surface cracks on the machined specimens appear more pronounced and orderly oriented as compared to that on the LSG specimens. Many surface cracks on the machined specimen formed at an inclination of approximately 45° angle to the loading axis as shown in Figure 10(b). Some surface cracks initiated along the machining marks. In contrast, the orientation of surface cracks on the LSG specimen is more random and not associated with the grinding traces. Machining traces on the specimen surface can give rise to stress concentration and promote crack initiation during tensile testing in hydrogen.[9,27] Therefore, the presence of machining traces on the specimen surface is believed to be one of the mechanisms that contribute to the reduced tensile fracture elongation in hydrogen.

The tensile behavior in hydrogen is quite different from that in air. Surface cracks are present throughout the entire necked area of all specimens tested in hydrogen, which can be attributed to hydrogen-induced/assisted cracking that becomes more pronounced after macroscopic necking.[28] Formation of surface cracks on tensile specimens in the presence of hydrogen is caused by triaxial stress state that originates following necking.[29] Therefore, it is reasonable to assume that losses in ductility for LP-DED NASA HR-1 during very slow strain rate tensile testing in hydrogen (at 0.0005 in/in/min or slower) are primarily associated with accelerated surface crack initiation and growth after necking. This is consistent with the observations that more pronounced surface cracking corresponds to a higher degree of HEE susceptibility in both machined and LSG specimens when they were subjected to very slow strain rate tensile testing in hydrogen.

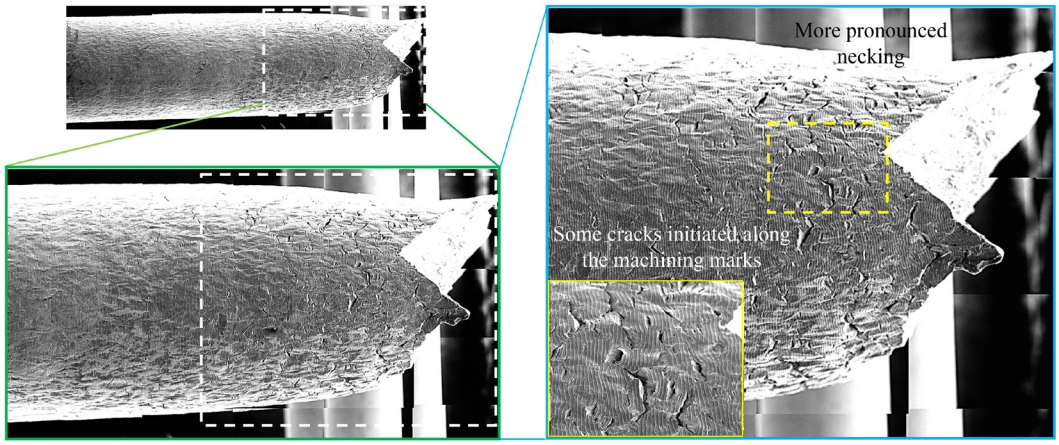

(a) Most surface cracks present near the facture surface.

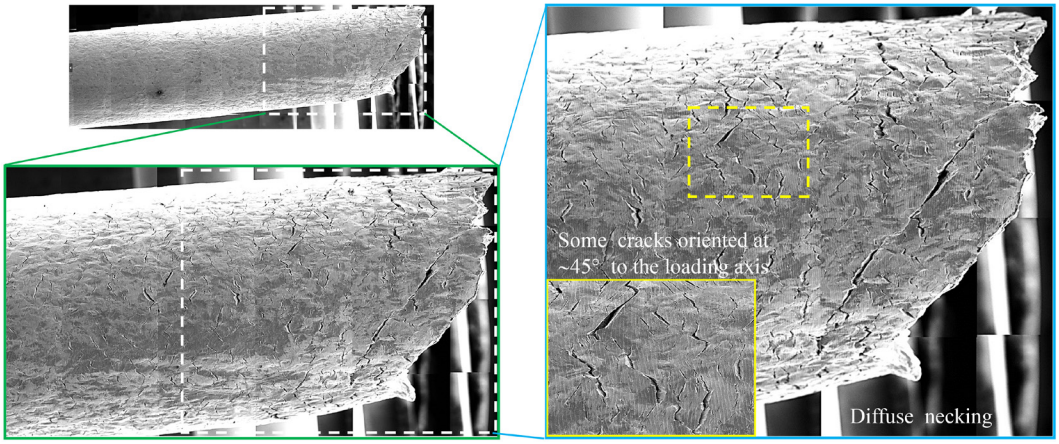

(b) Most surface cracks present near the facture surface.

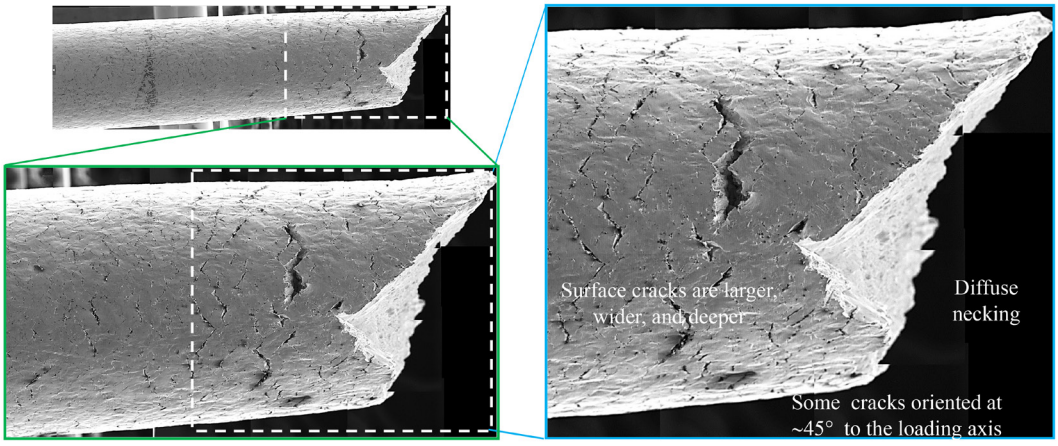

(c) Most surface cracks present near the facture surface.

Figure 10. SEM images showing surface cracking behavior of machined specimens tensile tested in hydrogen at the strain rate of (a) 0.005, (b) 0.0005, and (c) 0.0001 in/in/min. Three images are presented for each sample. Surface cracks became wider and longer when the strain rate is reduced from 0.005 to 0.0005 in/in/min or slower.

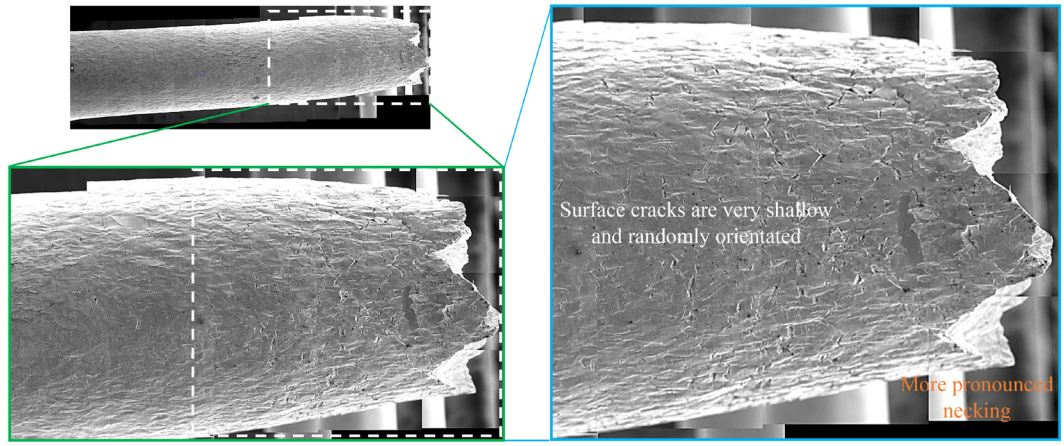

(a) Most surface cracks present near the facture surface.

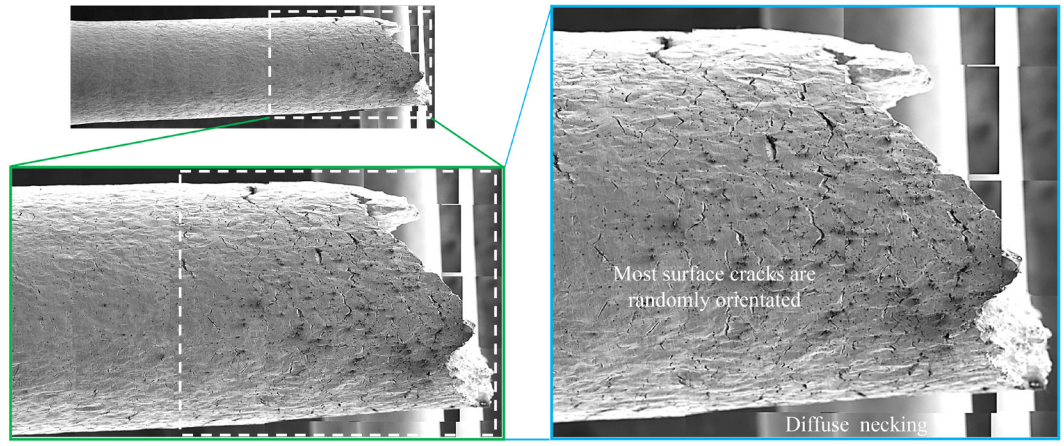

(b) Most surface cracks present near the facture surface.

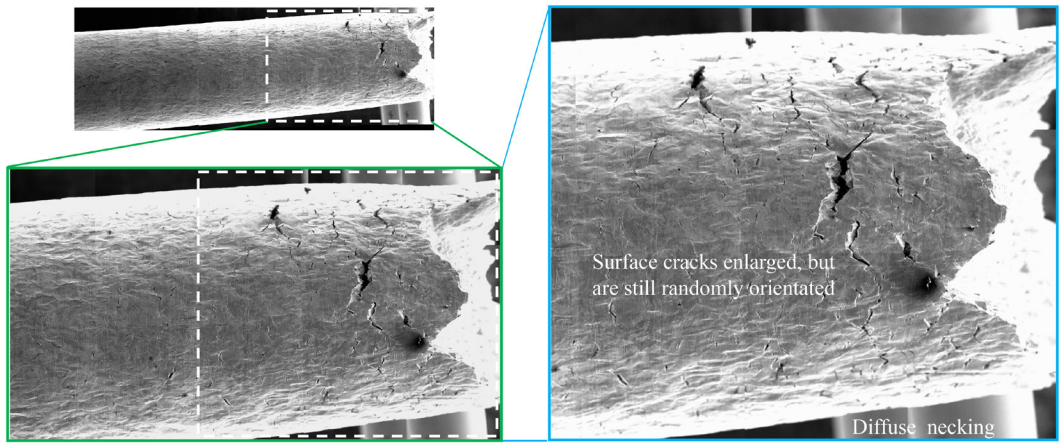

(c) Most surface cracks present near the facture surface.

Figure 11. SEM images showing surface cracking behavior of LSG specimens tensile tested in hydrogen at the strain rate of (a) 0.005, (b) 0.0005, and (c) 0.0001 in/in/min. Three images are presented for each sample. Surface cracks became wider and longer when the strain rate is reduced from 0.005 to 0.0005 in/in/min or slower.

3.7 Depth of Surface Crack Analysis

An in-depth analysis on the depth of surface cracks was performed to see the effects of strain rate and surface finish condition on hydrogen-induced surface cracking behavior. Cross-sectional images of broken tensile specimens with two surface finish conditions and tested at three strain rates in hydrogen are shown in Figures 12 and 13. The depth of surface cracks are compared at two locations for each specimen, roughly 0.15 inches from the fracture surface and the vicinity of the specimen shoulder. Both machined and LSG specimens have visible surface cracks after tensile testing at 0.005 in/in/min in hydrogen. Most surface cracks are shallow, approximately 10–40 μm deep. Signs of plastic deformation can be clearly seen in the specimen shoulder region, which indicates the material remains very ductile in hydrogen and plastic deformation extended outside the specimen gauge. The fracture surface exhibits predominant shear-dominate ductile transgranular type of fracture at approximately 45° to the loading axis.

The depth and number of surface cracks increases significantly with decreasing strain rate to 0.0005 as shown in Figures 12(b) and 13(b). The degree of surface cracking on the machined specimen is higher than that on the LSG specimen. Most surface cracks are approximately 20–60 μm deep on the machined specimen and 10–50 μm deep on the LSG specimen. However, there are a few deep surface cracks up to 100 μm deep near the specimen shoulder region on the machined specimen. In comparison, surface cracks are significantly smaller and fewer near the specimen shoulder region on the LSG. In both machined and LSG specimens, the majority of surface cracks grew along the plane of maximum shear, and they are oriented at approximately 35–45° with respect to the tensile loading direction. This demonstrates that LP-DED NASA HR-1 remains very ductile in high pressure hydrogen environment as surface cracks initiated by ductile shear mode.

The depth of surface cracks increased further when tensile tests were performed at a very slower strain rate of 0.0001 in/in/min in hydrogen as shown in Figures 12(c) and 13(c). The LSG specimens exhibit fewer surface cracks than the machined specimens and they are shallower and more randomly distributed. The deepest surface cracks in the machined and LSG specimen were on the order of 140 μm and 80 μm, respectively. It must be noted that several sizeable surface cracks up to 100 μm deep are present near the shoulder region of the machined specimen. In comparison, the deepest surface crack on the LSG specimen shoulder region is about 30 μm deep, which is significantly shallower than that in the machined specimen. Since the surface roughness is comparable for the machined and LSG specimens, the difference in the surface cracking behavior between them is likely caused by the difference in the magnitude of residual stress on the specimen surface. Residual stress can be easily introduced to the specimen surface during final machining by turning. In contrast, low stress grinding (LSG) can reduce surface residual stress to a very low level.

There is a correlation between the surface residual stress and hydrogen content as tensile residual stress expands the crystal lattice and promotes hydrogen entry, diffusion, and absorption.[30] In contrast, compressive residual stress mitigates stress concentration around a crack tip due to the crack closure effect and decreased hydrogen concentration around the crack tip. It has been reported that hydrogen has a tendency to concentrate around a crack tip, where hydrostatic stress is high, and penetrates deep into the material along with the propagating crack tip.[3] Therefore, the residual stress field near the specimen surface is expected to play a significant role

in hydrogen diffusion and absorption behaviors.[30] After final machining by turning, the residual stress is tensile at the surface and compressive below the surface for machined Inconel 718.[31] As a result, the residual stress distributions on the surface of machined LP-DED NASA HR-1 tensile specimens are expected to be tensile in nature. Therefore, it is postulated that the presence of higher tensile residual stress on the machined surface contributes to the observed differences in surface cracking behavior and tensile ductility degradation in hydrogen between the machined and LSG specimens. This explains why the machined surface is more susceptible to HEE than the LSG surface.

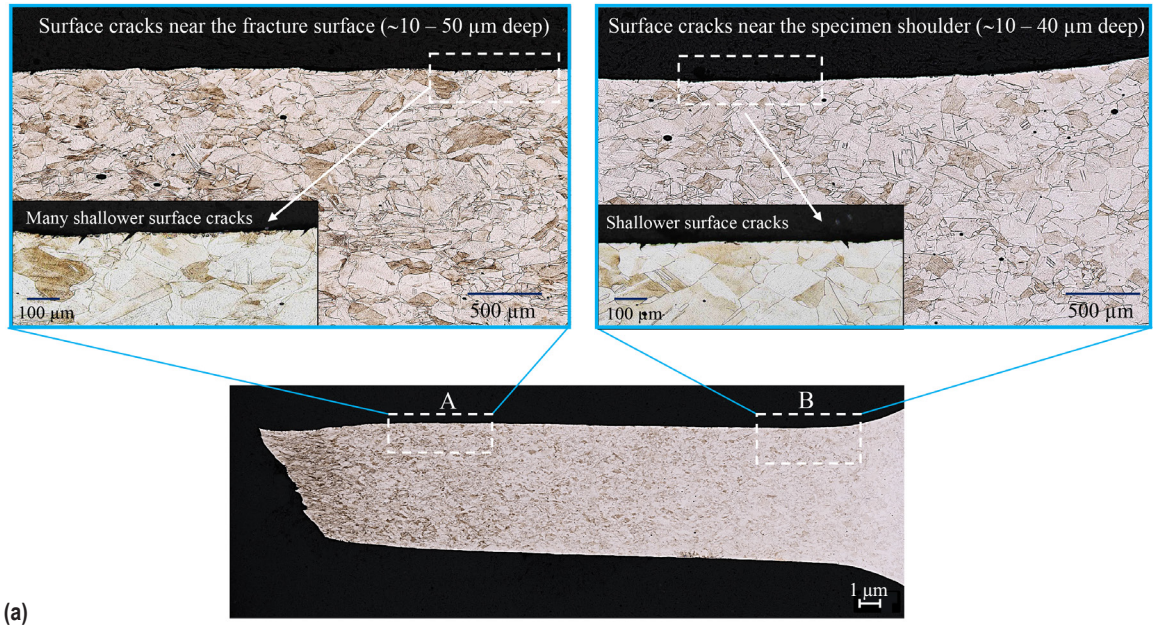

(a)

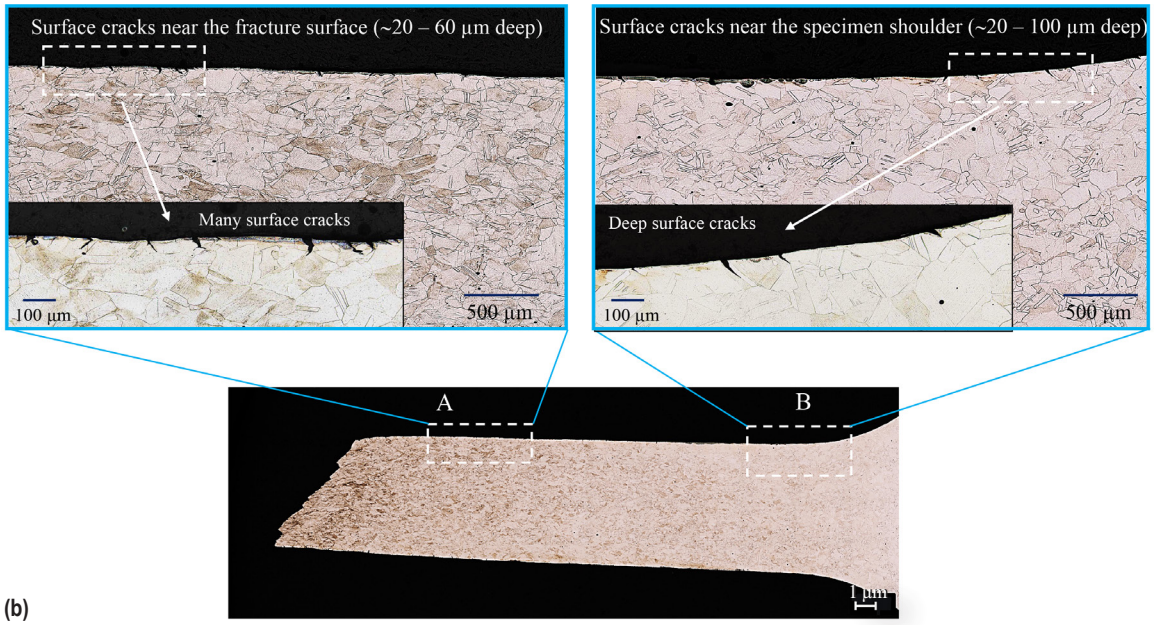

(b)

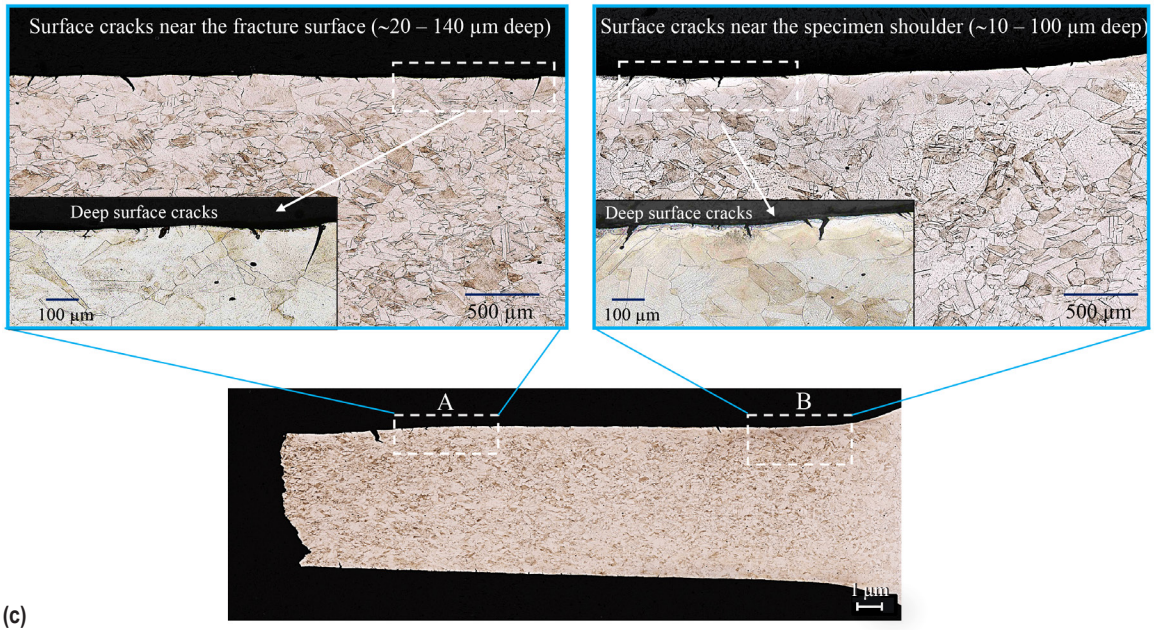

Figure 12. Optical images showing cross-sectional views of fractured tensile specimens (with machined surface finish) tested in hydrogen at the strain rate of (a) 0.005, (b) 0.0005, and (c) 0.0001 in/in/min. Five images are presented for each sample. Most surface cracks are oriented at approximately 35–45° with respect to the loading direction. The surface cracking mode is predominantly ductile transgranular.

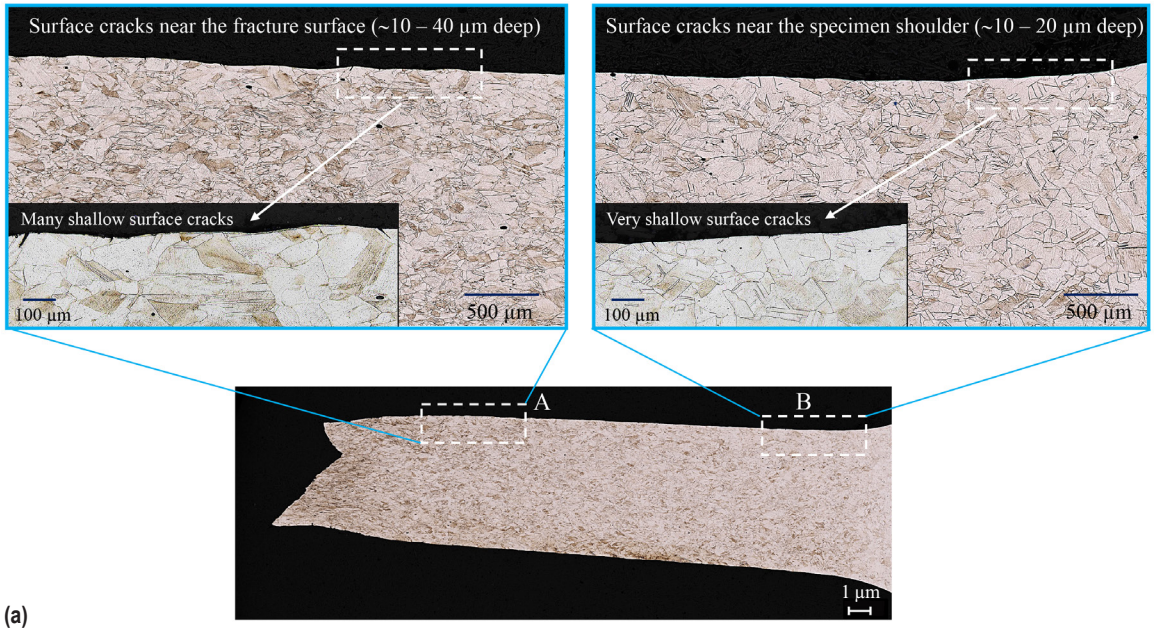

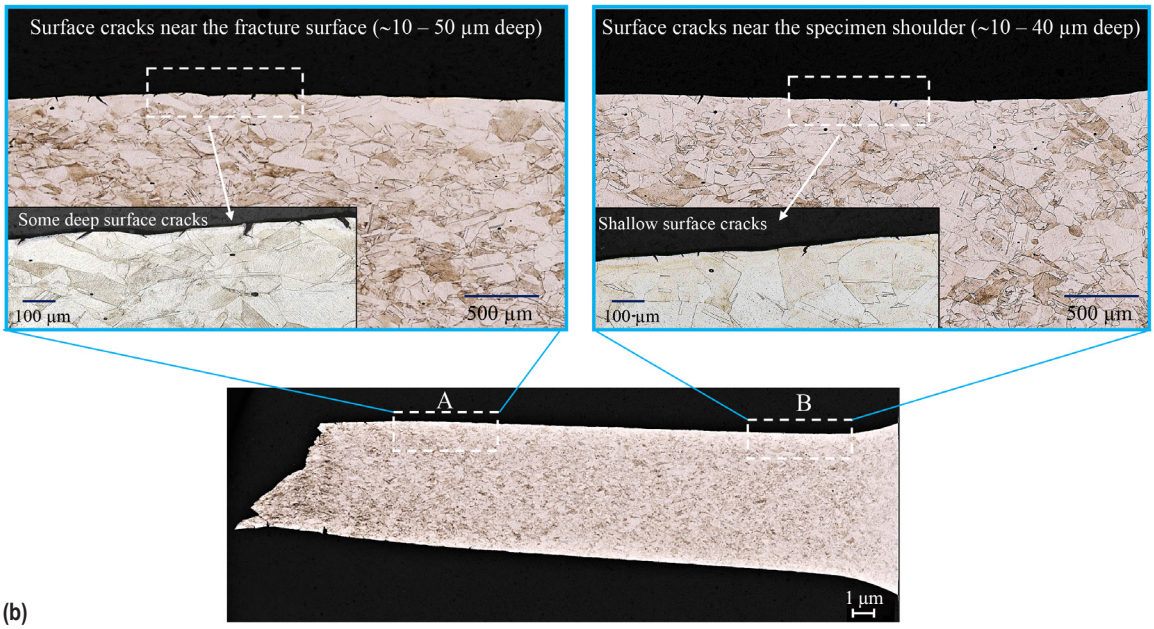

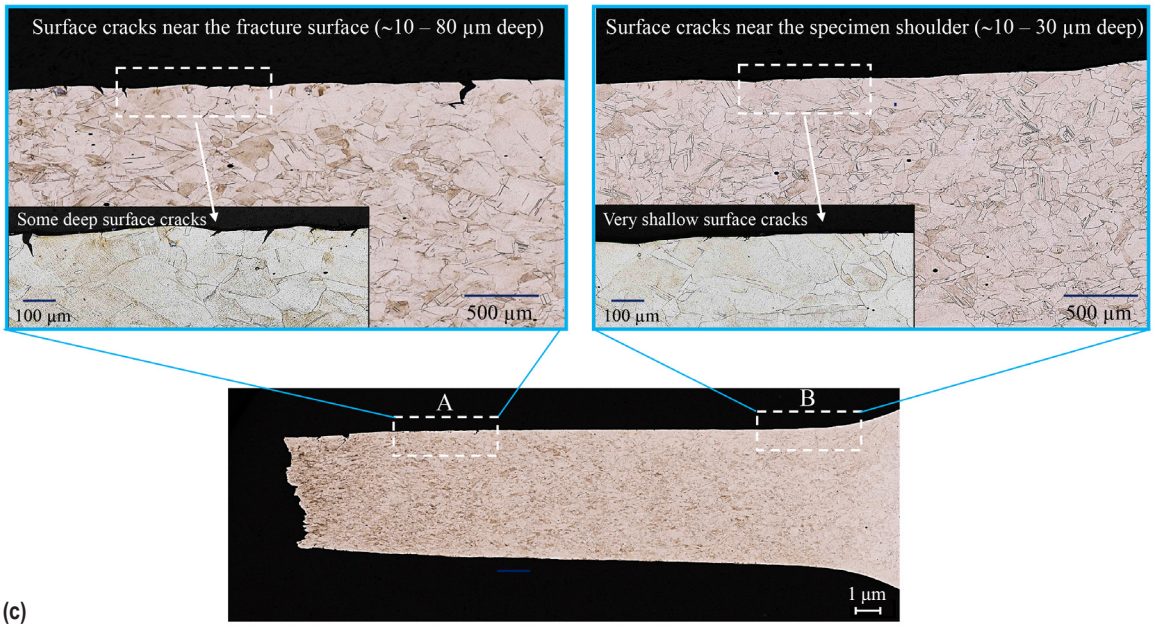

Figure 13. Optical images showing cross-sectional views of fractured tensile specimens (with LSG surface finish) tested in hydrogen at the strain rate of (a) 0.005, (b) 0.0005, and (c) 0.0001 in/in/min. Five images are presented for each sample. Most surface cracks are oriented at approximately 35–45° with respect to the loading direction. The surface cracking mode is predominantly ductile transgranular.

3.8 Strain Rate Effect on Hydrogen Diffusion

Hydrogen influences surface crack initiation and hydrogen-induced cracks start at the gas-metal surface.[32] In alloy 718, the resistance to HEE is related to hydrogen diffusion behavior, and hydrogen transport by diffusion is an important consideration for interpreting the susceptibility to HEE.[33] The depth of hydrogen diffusion in LP-DED NASA HR-1 can be estimated using the bulk diffusivity for hydrogen in alloy 718 at room temperature, which is on the order of 2×10^{-15} m^2/s.[3] The diffusion distance of hydrogen has a square root dependence on diffusivity and can be determined from the equation below:[34]

$$x = \sim (Dt)^{1/2}$$

where x is the diffusion distance traveled by the diffusing hydrogen atoms in one direction along one axis, D is diffusivity, and t is the elapsed time since diffusion began. The diffusivity determines the time it takes for a hydrogen atom to diffuse a given distance in an alloy.

The tensile test strain rate for LP-DED NASA HR-1 in hydrogen varies from 0.005 to 0.0001 in/in/min. The variation in strain rate changes the testing duration in hydrogen from 25–35 minutes (at 0.005 in/in/min) to as high as 800–900 minutes (at 0.0001 in/in/min). When a tensile test is performed at a strain rate of 0.005 in/in/min for 25–35 minutes, hydrogen atoms absorbed on the specimen surface can diffuse over a very short distance of approximately 1.73–2.05 μm. This indicates the potential for hydrogen assisting in the failure process is lower at 0.005 in/in/min, since the distance it can diffuse during tensile testing is very limited. In comparison, when the strain rate is decreased to 0.0001 in/in/min, the exposure time in hydrogen environment increases to more than 800–900 minutes (23× time), and the estimated depth of hydrogen diffusion at the failure would increase from 1.73–2.05 μm to approximately 9.80–10.39 μm. It is apparent that the fraction of deforming material that is affected by hydrogen is considerably larger at 0.0001 in/in/min than at 0.005 in/in/min due to the difference in the exposure time in hydrogen. This explains why HEE sensitivity increased when tensile tests were run at very slow strain rates due to increased depth of hydrogen diffusion, which would promote interaction of hydrogen and the moving dislocations.[3,5,6,34]

Although the calculated hydrogen diffusion distance is significantly shorter than the measured depth of surface cracks, a clear trend of increasing depth of surface cracks with decreasing strain rate can be observed. The actual surface cracks being deeper than the calculated hydrogen diffusion distance represent an area where hydrogen transportation can be assisted by moving dislocations beyond the limit of lattice diffusion.[35] At a higher strain rate, the diffusion of hydrogen may not be able to follow the dislocation motion, leading to a shallow penetration of hydrogen inside the specimen surface.[5] In contrast, hydrogen can diffuse deeper and follow the slow dislocation motion when the strain rate is decreased to a very low level. Therefore, the interaction of hydrogen with dislocation is enhanced and a higher amount of hydrogen can be effectively transported by dislocations to the high stress regions when the strain rate is below a certain threshold value. The high pressure hydrogen environment continues to supply hydrogen to the near-surface dislocation sources. Mobile dislocations draw hydrogen inward at a rate significantly higher than that allowed by normal lattice diffusion. Towards the end of the tensile test, cracks are formed, and hydrogen can either diffuse or be transported by dislocations to the crack tip and accelerate the hydrogen induced failure.

3.9 Effects of Hydrogen on Fracture Behavior

Fracture surfaces were analyzed using SEM to explore the effects of hydrogen on tensile fracture behavior. Fractographic details and tensile failure mode of LP-DED NASA HR-1 tested under three strain rates in hydrogen are shown in Figures 14 and 15. Three images are presented for each sample, including the overall fracture surface, the hydrogen affected zone near surface, and a higher resolution image showing the mixed quasi-cleavage and dimple fracture in the hydrogen affected zone. As shown in Figures 14(a) and 15(a), both machined and LSG specimens display similar fracture characteristics after tensile testing at the strain rate of 0.005 in/in/min in hydrogen. There is a small hydrogen affected zone around the circumference of the fracture surface in the machined and LSG specimens. Higher resolution SEM images reveal the hydrogen affected zone has mostly ductile dimple type of fracture with a few very small hydrogen-induced cracks. It is apparent that hydrogen has little influence on tensile fracture behavior of LP-DED NASA HR-1 when tensile testing was conducted at the standard strain rate of 0.005 in/in/min.

The fracture surface morphology looks significantly different when the strain rate was reduced to 0.0005 in/in/min. Figures 14(b) and 15(b) display the SEM images of a machined and a LSG specimen tensile tested in hydrogen at 0.0005 in/in/min. The fracture surface morphology of the machined and LSG specimens look similar with no distinct differences. There are two to three hydrogen affected zones that can be clearly identified on the fracture surface. At 0.0005 in/in/min, the hydrogen induced cracks become larger and exhibit more distinct quasi-cleavage facet morphology. The quasi-cleavage fracture surface is flatter and mixed with secondary cracks and traces of ductile dimples. Outside of the hydrogen affected zones, a more ductile mode of failure occurs, and ductile-dimple type of fracture is dominant. The ductile-dimple failure is representative of an overload mode of failure of the remaining ligament that is not affected by hydrogen. Based on the fractographic analysis, the hydrogen affected failure mode is surface crack formation, followed by crack growth, and eventually ductile "overload" failure. Although there are a few hydrogen affected quasi-cleavage regions on the fracture surface, LP-DED NASA HR-1 remains very ductile and have more than 33% fracture elongation after tensile testing for 8–9 hours in hydrogen.

The depth of the less ductile quasi-cleavage zone varied significantly with the strain rate. When strain rate was reduced to 0.0001 in/in/min, the depth of hydrogen affected quasi-cleavage zone extended deeper and covered a sizeable portion of the fracture surface as shown in Figures 14(c) and 15(c). This phenomenon is expected because the testing duration in hydrogen increases drastically with decreasing strain rate. The increased depth of hydrogen-induced quasi-cleavage fracture was likely caused by hydrogen being transported deeper into the specimen as the crack continued to propagate during lengthy testing in hydrogen.[33] Although the hydrogen affected zone becomes much larger and deeper when the strain rate is reduced from 0.0005 to 0.0001 in/in/min, it is significant to note that the fracture elongation does not decrease further. This phenomenon can be attributed to the growth rate of hydrogen-induced cracks being extremely slow when a single tensile test lasted for 13–15 hours at 0.0001 in/in/min. As a result, further reduction in fracture elongation was prevented as the extremely slow test speed delayed the overload failure and permitted the hydrogen affected zone to grow slowly and cover a sizeable portion of the fracture surface before the final fracture.

From the fractographic analysis, it is evident that the interaction of external gaseous hydrogen with the tensile specimen is initially confined within its outer region during tensile testing. Surface cracks initiated from the circumference and continued to grow inward. The failure of tensile specimens in hydrogen started with surface crack formation, followed by crack growth, and eventually ductile overload failure. Hydrogen embrittlement is undoubtedly more pronounced at slow strain rates as the hydrogen-induced quasi-cleavage facets become larger and more distinct. Hydrogen concentration at the crack tip can be greatly influenced by strain rate.[36] Hydrogen can follow the slow-moving dislocations to the stress concentration sites when the strain rate is very slow.[3,5,37] Hydrogen was transported deep into the material towards the end of the slow strain rate tensile test, leading to reduced fracture elongation. Intergranular fracture, which is the most severe form of HEE, is not present on the fracture surface of LP-DED NASA HR-1.

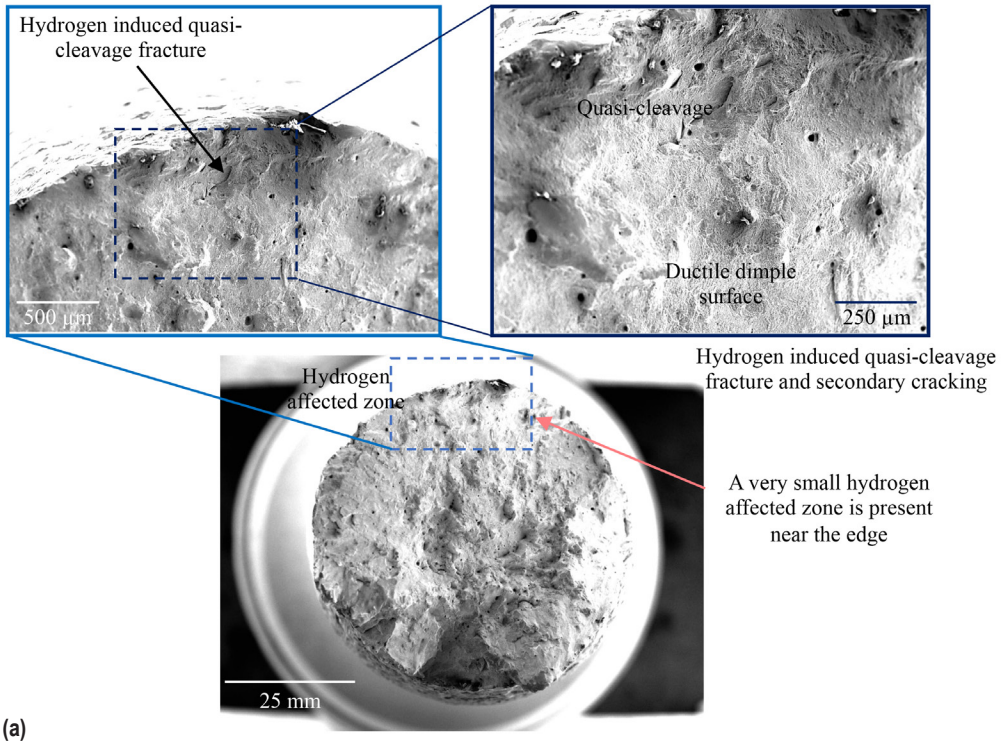

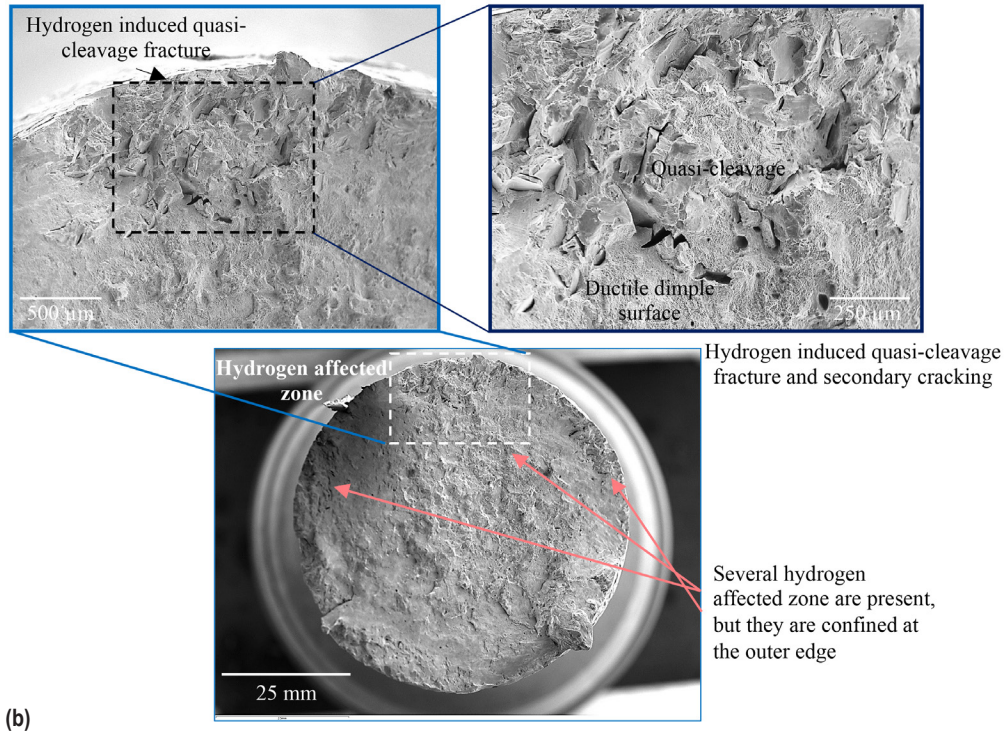

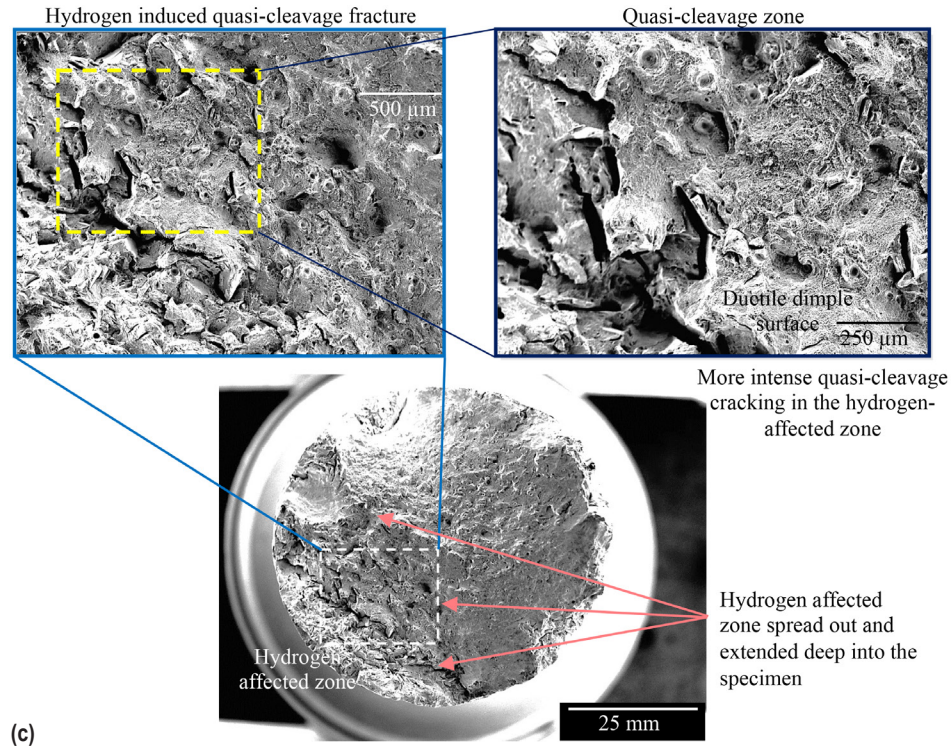

Figure 14. SEM fractography of machined specimens tensile tested in hydrogen at the strain rate of (a) 0.005, (b) 0.0005, and (c) 0.0001 in/in/min. Three images are presented for each sample to show the overall fracture surface, the HEE affected zone near the specimen surface, and hydrogen-induced quasi-cleavage fracture.

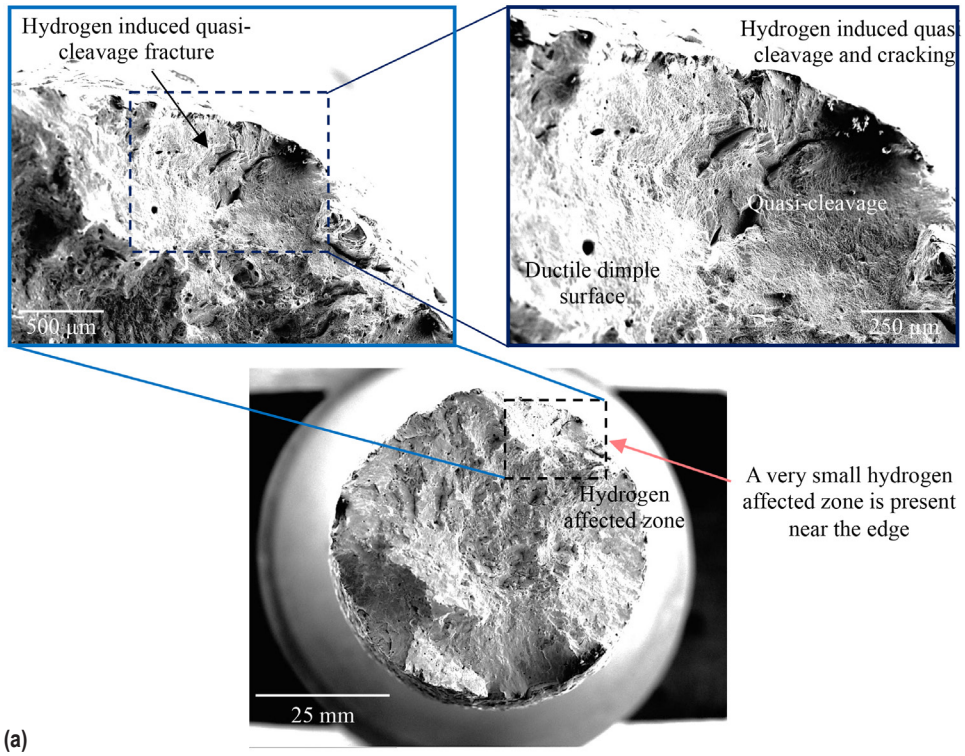
Hydrogen induced quasi-cleavage fracture
500 µm
Hydrogen induced quasi-cleavage and cracking
Quasi-cleavage
Ductile dimple surface
250 µm
Hydrogen affected zone
A very small hydrogen affected zone is present near the edge
25 mm

(a)

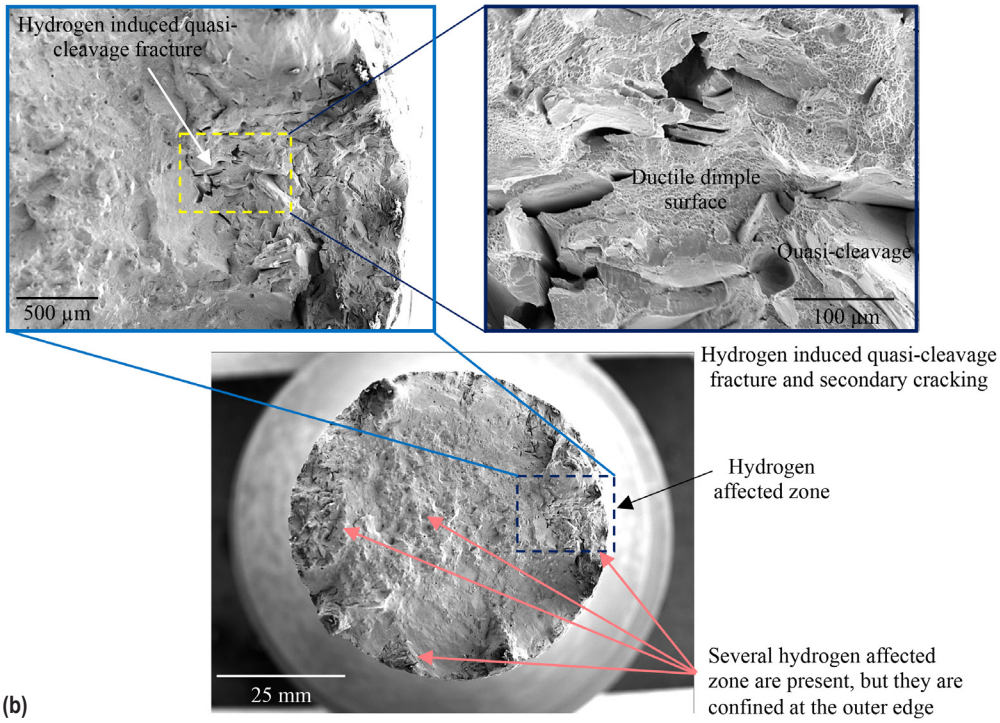
Hydrogen induced quasi-cleavage fracture
500 µm
Ductile dimple surface
Quasi-cleavage
100 µm
Hydrogen induced quasi-cleavage fracture and secondary cracking
Hydrogen affected zone
Several hydrogen affected zone are present, but they are confined at the outer edge
25 mm

(b)

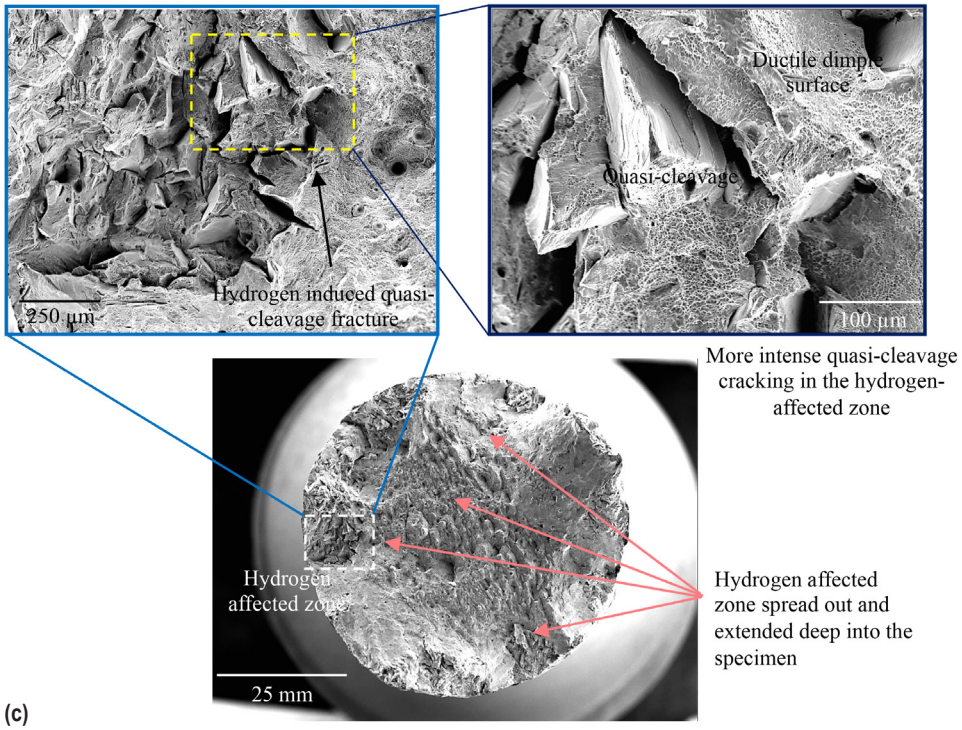

Figure 15. SEM fractography of LSG specimens tensile tested in hydrogen at the strain rate of (a) 0.005, (b) 0.0005, and (c) 0.0001 in/in/min. Three images are presented for each sample to show the overall fracture surface, the HEE affected zone near the specimen surface, and hydrogen-induced quasi-cleavage fracture.

3.10 Suitability of Slow Strain Rate Tensile Testing for HEE Screening

Smooth tensile testing in hydrogen is intended to provide a reasonably rapid material screening to qualitatively evaluate the susceptibility of HEE, instead of determining the effects of long- term exposure in a hydrogen service environment. There are a few factors that can affect the HEE screening results and data interpretation when the strain rate is very slow. Table 8 summarizes the effects of strain rate on tensile testing duration, hydrogen (H) diffusion distance, depth of surface cracks, hydrogen embrittlement (HE) category, and fracture driving force. As shown in Table 8, decreasing strain rate significantly increases testing duration, hydrogen diffusion distance, and depth of surface cracks. A couple of technical complications may arise from very slow strain rate tensile testing and make evaluation of HEE screening results difficult and complex. First, the distance of hydrogen diffusion increases by roughly a factor of 5, form 1.73–2.05 µm to 9.8–10.39 µm when the strain rate is decreased from 0.005 to 0.0001 in/in/min. The depth of hydrogen diffusion can increase further when the material is subjected to persistent high tensile stresses (close to the UTS) as stress can expand the crystal lattice and promote hydrogen diffusion.[30] The increased diffusion time in conjunction with stress-assisted diffusion permit hydrogen to diffuse deep into the material, which may result in some degree of Internal Hydrogen Embrittlement (IHE), in addition to HEE. IHE, a more severe form of hydrogen embrittlement than HEE, can

be regarded as the embrittlement of a material due to introduction of hydrogen into the materials under an applied stress.[2] The combined effects of HEE and a certain degree of IHE from very slow strain rate tensile screening testing is expected to show more severe HEE than would be encountered in service. In contrast, IHE is not expected to be a factor when HEE screening tests are performed at 0.005 in/in/min as the time for hydrogen absorption and diffusion from the surface into the material is short (25–35 minutes).

Table 8. Effects of strain rate on tensile testing duration, hydrogen diffusion distance, depth of surface cracks, HE category, and fracture driving force. IHE denotes internal hydrogen embrittlement. The depth of surface cracks were measured from the machined specimens at roughly 0.15 inches from the fracture surface and in the vicinity of the specimen shoulder.

Material	Media	Strain rate (in/in/min)	Testing Duration (min)	H Diffusion Distance (μm)	Depth of Surface Cracks (μm)	HE Category	Fracture Driving Force
LP–DED NASA HR–1 (machined finish)	5 ksi GH_2	0.005	25 – 35	1.73 – 2.05	10 – 50	HEE	Tensile
		0.0005	500 – 600	7.75 – 8.49	20 – 100	HEE + IHE	Tensile + crack growth
		0.0001	800 – 900	9.80 – 10.39	20 – 140	HEE + IHE	Tensile + crack growth

The other technical complication associated with very slow strain rate tensile testing is the slow dynamic strain would promote growth of surface cracks during lengthy tensile testing in hydrogen. As shown in Table 8, growth of surface cracks was enhanced when the strain rate was very slow. The depth of hydrogen-induced surface cracks increased considerably from 10-50 μm at 0.005 in/in/min to 20–140 μm at 0.0001 in/in/min. The depth of surface cracks are compared at two locations for each specimen, roughly 0.15 inches from the fracture surface and in the vicinity of the specimen shoulder as shown in Figure 12. A tensile test is no longer a normal tensile test when fracture is assisted by crack growth.[3,38] As a result, a HEE screening tensile test performed with a cracked specimen becomes a complex test of combined tensile and crack growth, which can influence the tensile properties in hydrogen (see Table 8). Under such circumstance, the applied tensile stress is no longer the only fracture driving force as the fracture process can be assisted by crack growth, which is dependent on the stress intensity factor (K) near the tip of a crack. A fracture mechanics-based approach is required to analyze the effects of stress intensity on crack growth, fracture elongation, and ultimate tensile stress.[39,40] The choice of tensile testing strain rate should be based on its ability to assess HEE susceptibility relative to in-service conditions and the test being reasonably rapid and reproducible. Very slow strain rate tensile testing at 0.0005 in/in/min or slower is unsuitable for HEE screening as the technical complications introduced by IHE and crack-growth assisted fracture make data analysis extremely difficult and unreliable.

3.11 Correlation of HEE Screening Test Results and LCF Life in Hydrogen

Mechanical property data other than tensile properties must be considered in designing components for LRE applications. Low cycle fatigue (LCF) is the life-limiting property for LRE nozzles.[13] Hydrogen can have significant effects on strain-controlled LCF life for HEE susceptible materials because the effects of hydrogen are primarily on plastic deformation and ductility. It has been demonstrated that the HEE susceptibility trend generated by smooth tensile screening testing correlates well with LCF behavior trend in hydrogen.[2] Therefore, the HEE screening results obtained from tensile testing can be used to assess the effects hydrogen on LCF behavior for LP-DED NASA HR-1. Figure 16 presents the HEE screening tensile test results obtained from this study (at 0.005 in/in/min) and the strain-controlled LCF test results at 2% total strain in hydrogen for LP-DED NASA HR-1.[13] As shown in Figure 16(a), LP-DED NASA HR-1 has excellent resistance to HEE when tested at 0.005 in/in/min. The %EL ratio (GH_2/GN_2) is 95% for the machined specimens and 103% for the LSG specimens. Effect of hydrogen on LCF life for LP-DED NASA HR-1 is shown in Figure 16(b). As shown, LCF life in hydrogen is comparable to that in air at 2% total strain. The typical LCF life is 827-1121 cycles in air and 878-893 cycles in hydrogen. It is proven again that running smooth tensile testing in hydrogen at 0.005 in/in/min is an effective screening method for HEE susceptibility evaluation as the screening results agree well with the LCF behavior in hydrogen. The excellent LCF performance in hydrogen makes LP-DED NASA HR-1 an ideal material for LRE structures that are subjected to repeated thermal and mechanical loads in the challenging high pressure hydrogen environment.[13] NASA has manufactured multiple components using LP-DED NASA HR-1 and successfully tested over 280 starts and 8,914 seconds in hydrogen environments on integral channel wall nozzles.[13]

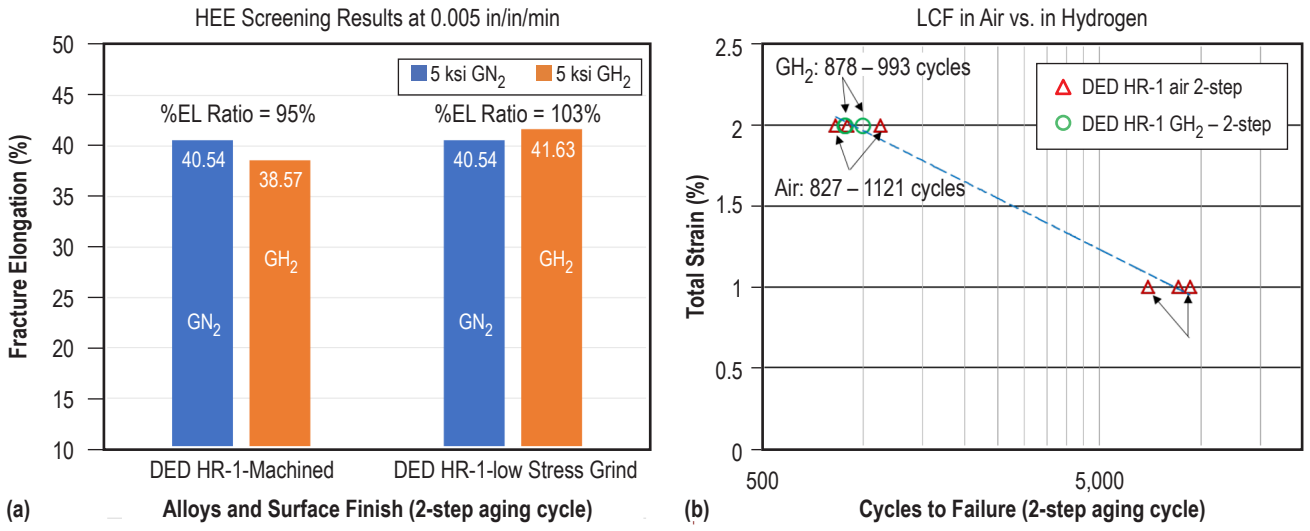

Figure 16. (a) HEE susceptibility screening test results obtained at 0.005 in/in/min and (b) the strain-controlled LCF test results at 2% total strain in hydrogen and air for LP-DED NASA HR-1.[13] The trend of HEE screening results by tensile testing correlates well with that of the strain-controlled LCF behavior in hydrogen.

4. RECOMMENDATIONS

Performing smooth tensile testing in hydrogen is a rapid screening method to determine the relative HEE susceptibility of materials. There are several factors that can influence tensile test results in high pressure hydrogen environment, including strain rate, specimen surface finish, test system, and material factors. The most significant HEE data variations among laboratories and different studies arise from inconsistency in test speed (strain rate) and specimen preparation (surface finish). The historic standard test speed at MSFC for smooth tensile testing in hydrogen has been the stoke rate that results in a pre-yield strain rate of 0.005 in/in/min. Performing smooth tensile testing in hydrogen at 0.005 in/in/min has been proven very effective for developing new alloys, screening, and qualifying candidate alloys for LRE applications. The standard strain rate of 0.005 in/in/min was used to develop a hydrogen resistant wrought alloy NASA HR-1 at MSFC, to qualify wrought JBK-75 for hydrogen service, and to perform HEE susceptibility screening tests for other candidate rocket propulsion materials.[16,23,1] HEE screening of candidate materials should take the service conditions into consideration to ensure the tests can adequately evaluate the potential of HEE in service. Running a smooth tensile test at a strain rate of 0.0005 in/in/min or slower is not suitable for HEE screening as the test data can be complicated by the presence of IHE and crack growth assisted tensile fracture.

Specimen surface finish condition also influences HEE susceptibility because the failure mode in hydrogen starts with surface crack formation. According to ASTM standard G142, specimens shall be machined by grinding to have a minimum amount of cold work on the gauge surface.[12] Final machining by turning generates machining traces and residual stress on the specimen surface that affect HEE susceptibility. Another concern with the use of turning method for final machining is the variation in the machining speed (material removal rate) can also affect HEE susceptibility. An increase in the machining speed has been shown to decrease hydrogen resistance for alloy 718, which is likely caused by an increase in the tensile residual stress on the surface.[8,41] Therefore, the method of final machining should be performed by grinding to avoid adding additional variables that influence HEE screening results. Based on the findings of this study, it is recommended that smooth tensile testing in hydrogen for HEE screening shall be performed at a pre-yield strain rate of 0.005 in/in/min using specimens with LSG surface finish. After HEE screening and qualification, other mechanical properties, such as LCF, crack growth (da/dn), and fracture properties, should be considered in designing components for service in high pressure hydrogen environment.

5. CONCLUSIONS

LP-DED NASA HR-1 was subjected to tensile tests by varying strain rate and surface finish under a 5 ksi high pressure hydrogen environment at room temperature, and the following findings were obtained.

(1) The HEE tensile screening results verified that NASA HR-1 in LP-DED form is an excellent material for use in liquid rocket engine applications, as it is very ductile and exhibits a high resistance to HEE. LP-DED NASA HR-1 with LSG surface finish exhibits no ductility loss when tested in hydrogen at the standard strain rate of 0.005 in/in/min. Machined samples have a slight 2% ductility reduction in hydrogen at the same strain rate. LP-DED NASA HR-1 exhibits comparable tensile ductility ratio to the wrought alloy at the strain rate of 0.005 in/in/min in hydrogen but is significantly more ductile than the wrought alloy.

(2) Hydrogen induced tensile ductility reductions are sensitive to strain rate and surface finish condition. Very slow strain rate tensile testing at 0.0005 in/in/min or slower is unsuitable for HEE screening as the technical complications introduced by IHE and crack-growth assisted fracture make data analysis extremely difficult and unreliable. The combined effects of IHE and crack growth assisted tensile fracture that occur during very slow strain rate tensile testing is expected to show more severe HEE susceptibility than would be encountered in service.

(3) The primary effect of hydrogen on tensile properties is on ductility (%EL) and not strength. The effect of strain rate and surface finish on yield and tensile strength for LP-DED NASA HR-1 is insignificant in hydrogen. Both LSG and machined samples exhibit no reduction in yield stress in hydrogen at all three strain rates. Ultimate tensile stress (UTS) appears to be slightly influenced in hydrogen at very slow strain rates, but the UTS ratios (GH_2/GN_2) are above 96% for all conditions.

(4) The baseline tensile test results in ambient air show that strain rates in the range of 0.01-0.0005 in/in/min have no effect on tensile properties for LP-DED NASA HR-1. The 5 ksi inert nitrogen gas pressure also has no noticeable effect on tensile properties.

(5) Based on the findings of this study, it is recommended that smooth tensile testing in hydrogen for HEE screening shall be performed at a pre-yield strain rate of 0.005 in/in/min using specimens with LSG surface finish. Performing smooth tensile tests at 0.0005 in/in/min or slower in hydrogen is not recommended for HEE screening and qualifying alloys of interest for LRE applications.

REFERENCES

1. Vesely, Jr., Edward J., Robert K. Jacobs, and Michael C. Watwood. "Influence of Strain Rate on Tensile Properties in High-pressure Hydrogen," Hydrogen Effects in Materials, edited by A.W. Thompson and N.R. Moody, *Minerals, Metals, and Materials Society (TMS)*, (1994).

2. Lee, Jonathan A. "Hydrogen Embrittlement", *NASA Technical Memorandum*, 2016-218602.

3. Kagay, B. J. "Hydrogen Embrittlement Testing od Alloy 718 for Oil and Gas Application," *Masters Theses, Colorado School of Mines,* (2016), http://hdl.handle.net/11124/170301.

4. Zhang, Z., G. Obasis, R. Morana, and M. Preuss. "Hydrogen assisted crack initiation and propagation in a nickel-based superalloy," *Acta Materialia* 113, 272-283. https://doi.org/10.1016/j.actamat.2016.05.003.

5. Kim, Y., Y. Kim, D. Kim, S. Kim, W. Nam, and H. Choe. "Effects of Hydrogen Diffusion on the Mechanical Properties of Austenite 316L Steel at Ambient Temperature," *Materials Transactions* 52, no. 3, (2011), 507–513.

6. Depover, T., A. Elmahdy, F. Vercruysse, P. Verleysen, and K. Verbeken. "Effect of Strain Rate on the Hydrogen Embrittlement of a DP Steel," *EPJ Web of Conferences* 183, 03015, (2018).

7. Sakiyama, Y., T. Omura, K. Sugita, M. Mizuno, H. Araki, and Y. Shira. "Effect of Strain Rate on Hydrogen Embrittlement Susceptibility of Tempered Martensitic Steel," Proceedings of the 5th International Symposium on Steel Science (ISSS 2017). Kyoto, Japan: The Iron and Steel Institute of Japan (Nov. 13–16, 2017).

8. Bond, R., M. Watwood, and E. Vesley, Jr.. "The Effect of machining Techniques, Notch Design, and Strain Rates on the Notched Tensile Strength of Inconel 718 in high pressure Hydrogen," *Second Workshop on Hydrogen effects on materials in Propulsion systems* in *NASA Conference Publication* 3182, (1992).

9. Wada, Y., R. Ishigaki, Y. Tanaka, T. Iwadate and K. Ohnishi. "Evaluation of Metal Materials for Hydrogen Fuel Stations," Proceedings of the 1992 Annual Meeting of JSME/MMD, (November 2005), DOI:10.1299/jsmezairiki.2005.0_185.

10. Toribioa, J., M. Lorenzob, D. Vergaraa, V. Kharina. "Effects of Manufacturing-Induced Residual stresses and Strains on Hydrogen Embrittlement of Cold Drawn Steels," *Procedia Engineering* 10 (2011), 3540–3545.

11. Takakuwa, O., Y. Mano, H. Soyama. "The Interaction between Hydrogen and Surface Stress in Stainless Steel," *International Journal of Materials and Metallurgical Engineering* 8, no. 12 (2014).

12. ASTM G142-98. "Standard Test Method for Determination of Susceptibility of Metals to Embrittlement in Hydrogen Containing Environments at High Pressure, High Temperature, or Both," *ASTM International*. West Conshohocken, PA (2000) (R 2011), www.astm.org.

13. Chen, Po-Shou, Colton C. Katsarelis, William M. Medders, Paul R. Gradl, and Ching-Hua Su. "Development of Directed Energy Deposited NASA HR-1 to Optimize Properties for Liquid Rocket Engine Applications," NASA/TM, to be published in 2023.

14. Katsaleris, Colton C., Po-Shou Chen, Paul R. Gradl, Christopher S. Protz, Z. Jones, D. Ellis, and L. Evans. "Additive Manufacturing of NASA HR-1 for Liquid Engine Component Applications", *JANNAF*, (December 2019) United States.

15. Gradl, Paul R., Thomas W. Teasley, Christopher S. Protz, Colton C. Katsarelis, and Po-Shou Chen. "Process Development and Hot-fire Testing of Additively Manufactured NASA HR-1 for Liquid Rocket Engine Applications," *AIAA Propulsion and Energy Forum* (2021).

16. Chen, Po-Shou, Binayak Panda, and Biliyar N. Bhat. "NASA HR-1, A New Hydrogen Resistant Fe-Ni Base Superalloy", *Hydrogen Effects in Materials*, edited by A.W. Thompson and N.R. Moody, *Minerals, Metals, and Materials Sciety (TMS)*, (1994).

17. Gradl, Paul R., Darren C. Tinker, Alison Park, Omar R. Mireles, Marissa Garcia, Ryan Wilkerson, and Christopher McKinney. "Robust Metal Additive Manufacturing Process Selection and Development for Aerospace Components," *Journal of Materials Engineering and Performance*. Springer (2021). https://doi.org/10.1007/s11665-022-06850-0.

18. Gradl, Paul R. "Rapid Fabrication Techniques for Liquid Rocket Channel Wall Nozzles." AIAA-2016-4771, Paper presented at 52nd AIAA/SAE/ASEE Joint Propulsion Conference, July 27, 2016. Salt Lake City, UT.

19. Gradl, Paul R., and Christopher S. Protz."Technology advancements for channel wall nozzle manufacturing in liquid rocket engines," *Acta Astronautica* 174 (2020): 148-158 https://doi.org/10.1016/j.actaastro.2020.04.067.

20. Gradl, Paul R., Sandy E. Greene, William Brandsmeier, and Ian Johnston."Hot-fire Testing and Large-scale Deposition Manufacturing Development Supporting Liquid Rocket Engine Channel Wall Nozzle Fabrication," Paper presented at 65th JANNAF Propulsion Meeting/10th Liquid Propulsion Subcommittee, May 21–24, 2018. Long Beach, CA.

21. Gradl, Paul R., Sandy E. Greene, Christropher S. Protz, Brad Bullard, James Buzzell, Chance Garcia, Jessica Wood, Robin Osbourne, James Hulka, and Kenneth Cooper. "Additive Manufacturing of Liquid Rocket Engine Combustion Devices: A Summary of Process Developments and Hot-Fire Testing Results," *54th AIAA/SAE/ASEE Joint Propulsion Conference*. Cincinnati, OH: AIAA Propulsion and Energy Forum, July 9-12, 2018. AIAA 2018–4625.

22. Gradl, Paul R., Christopher S. Protz, and Tal Wammen. "Additive Manufacturing Development and Hot-fire Testing of Liquid Rocket Channel Wall Nozzles using Blown Powder Directed Energy Deposition Inconel 625 and JBK-75 Alloys," *55th AIAA/SAE/ASEE Joint*

Propulsion Conference. Indianapolis, IN: AIAA Propulsion and Energy Forum, August 19-21. AIAA-2019-4362.

23. Gibson, V. A., D. P. Dennis, and R. M. Horn. "Assessment of Candidate Rocket Propulsion materials in a Gaseous Hydrogen Environment," ed. *Second Workshop on Hydrogen effects on materials in Propulsion systems* of *NASA Conference Publication* 3182 (1992).

24. Gradl, P. R., A. Cervone, and E. Gill. 2022. "Surface texture characterization for thin-wall NASA HR-1 Fe–Ni–Cr alloy using laser powder directed energy deposition (LP-DED)." *Advances in Industrial and Manufacturing Engineering* 4, 100084. https://doi.org/10.1016/j.aime.2022.100084.

25. Carrez, P., and P. Cordier. "Plastic Deformation of Materials under pressure," *MRS Bulletin* 42 (October 2017).

26. Lewandowski, J. J., and P. Lowhaphandu. "Effects of Hydrostatic Pressure on Mechanical Behavior and Deformation Processing of Materials," *International Materials Reviews* 43, no. 4 (1998): 145.

27. Gao, T., Z. Sun, H. Xue, E. Bayraktar, Z. Qin, B. Li, and H. Zhang. "Effect of Turning on the Surface Integrity and Fatigue Life of a TC11 Alloy in Very High Cycle Fatigue Regime," *Metals* 10, (2020): 1507; doi:10.3390/met10111507.

28. Rao, G. S., Y. Yagodzinskyy, Z. Quea, P. Spätig, and H. P. Seifert. "Study on hydrogen embrittlement and dynamic strain ageing on low-alloy reactor pressure vessel steels," Journal of Nuclear Materials, Volume 556, 1 December 2021, 153161.

29. Nanninga, N., Y. Levy, E. Drexler, R. Condon, A. Stevenson, and A. Slifka. "Tensile Behavior of Pipeline Steels in High Pressure Gaseous Hydrogen Environments," *Materials Reliability Division*. Boulder, CO: National Institute of Standards and Technology: 80305

30. Takakuwa, O., Y. Mano, and H. Soyama. "The Interaction between Hydrogen and Surface Stress in Stainless Steel," *International Journal of Materials and Metallurgical Engineering* 8, no. 12, (2014).

31. Berruti, T., M. Lavella, and M. M. Gola. "Residual Stresses on Inconel 718 Turbine Shaft Samples after Turning," *Machining Science and Technology* (November 2009).

32. Michler, T., K. Wackermann, and F. Schweizer. "Review and Assessment of the Effect of Hydrogen Gas Pressure on the Embrittlement of Steels in Gaseous Hydrogen Environment," *Metals* 11, no. 4 (2021): 637, https://doi.org/10.3390/met11040637

33. Li, X., Q. Li, T. Wang, and J. Zhang. "Hydrogen-assisted failure in Inconel 718 fabricated by laser powder bed fusion: The role of solidification substructure in the embrittlement," Scripta Materialia 207, (15 January 2022): 114308

34. Marchi, C. S. "Gaseous Hydrogen Embrittlement of High Performance Metals in Energy System," ed. *Gaseous Hydrogen Embrittlement of Materials in Energy Technologies Mechanisms, Modelling and Future Developments.* Vol. 1 of *Metals and Surface Engineering*. Woodhead Publishing Series (2012), 471–484.

35. LaCoursiere, M.P., D.K. Aidun, and D.J. Morrison. "Slow Strain Rate Testing for Hydrogen Embrittlement Susceptibility of Alloy 718 in Substitute Ocean Water," *JMEPEG*, no. 26 (2017): 2337–2345, DOI: 10.1007/s11665-017-2675-x.

36. Fukunaga, A. "Slow Strain Rate Tensile Test Properties of Iron-Based Superalloy SUH660 in Hydrogen Gas," *ISIJ International* 59, no. 2 (2019), 359–366.

37. Bal, B., M. Koyama, G. Gerstein, H. J. Maier, and K. Tsuzaki. "Effect of Strain Rate on Hydrogen Embrittlement Susceptibility of Twinning-Induced Plasticity Steel Pre-charged with High-Pressure Hydrogen Gas," *International Journal of Hydrogen Energy* 41, no. 34 (14 September 2016), 15362–15372.

38. Chandler, W. T. "Hydrogen-Environment Embrittlement and Its Control in High Pressure Hydrogen/Oxygen Rocket System," *Advanced Earth-to-Orbit Propulsion Technology* of *NASA Conference Publication* 2437, no. 2, (1986).

39. Martínez-Pañeda, Emilio, Zachary D. Harris, Sandra Fuentes-Alonso, John R. Scully, and James T. Burns. "On the suitability of slow strain rate tensile testing for assessing hydrogen embrittlement susceptibility," *Corrosion Science*, no. 163, (February 2020), 108291.

40. Holroyd, N. Henry, T. L. Burnett, B. C. Palmer, and J. J. Lewandowski. "Estimation of environment-induced crack growth rate as a functionof stress intensity factors generated during slow strain rate testing of aluminum alloys", *Corrosion Reviews* 37, no. 5 (2019), 499–506.

41. Leppert, T., and R. L. Peng. "Residual stresses in surface layer after dry and MQL turning of AISI 316L steel," *Prod. Eng. Res. Devel.*, no. 6 (2012): 367–374, DOI 10.1007/s11740-012-0389–3.T.

National Aeronautics and
Space Administration
IS63
George C. Marshall Space Flight Center
Huntsville, Alabama 35812